



OPEN

# A yield design approach to the stability analysis of A seabed subjected to wave loading and pseudo-static seismic forces

João Paulo Chodacki Quiuqui &amp; Samir Maghous✉

The stability analysis of a seabed under the combined action of wave and seismic loading is investigated in the light of limit analysis theory and related static and kinematic approaches. Effects of cyclic wave loading are addressed in the context of the first-order Stokes theory, whereas the pseudo-static method is adopted to account for inertial forces induced in the seabed soil mass by earthquake events. Compared to existing works, the key contribution of the paper is two-fold: (i) incorporation of the destabilizing effects induced by the passage of seismic waves, and (ii) poromechanics-based evaluation of the pore pressure generated by the cyclic wave in the finite thickness seabed layer. Resorting to a total stress analysis, the stability condition of a purely cohesive seabed is formulated based on lower bound static and upper bound kinematic approaches, leading to closed-form expressions for seabed stability in terms of loading parameters or in terms of wave characteristics. For granular seabed soil, the stability analysis is handled within the framework of effective stress limit analysis reasoning in which the seepage flow related to pore pressure gradient can be accounted for by means of driven body forces. In that respect, particular emphasis is given to the decisive role of seepage forces that are derived from the pore pressure distribution associated with soil densification under the cyclic wave loading. Formulation of a seabed stability condition is then achieved by implementing the kinematic approach through a class of failure mechanisms, thus providing preliminary elements for assessing the influence of each loading component. Numerical simulations notably emphasized the destabilizing effects induced by seismic loading.

**Keywords** Seabed stability analysis, Waves and seismic loading, Seepage forces, Limit analysis, Total and effective stress analyses, Pseudo-static method

The growing interest in understanding seabed responses to wave impacts has been largely driven by the rapid development of marine structures and the increasing exploitation of offshore environments for energy generation, particularly through wind turbines<sup>1–3</sup>. In shallow waters or under intense wave conditions, wave-induced pressures on the seabed can cause significant soil displacements. Such phenomena are critical in coastal engineering as they can compromise the stability of offshore platforms and lead to the rupture of pipelines, underlining the need for thorough stability analyses of horizontal or inclined seabeds, even in cases where no structures are present.

Several mechanisms can be involved in seabed instability. According to Hance<sup>4</sup>, the main mechanisms cited in the literature include rapid sediment deposition, the presence of gas within the seabed, tidal events, human activities, erosion, sea level fluctuations, earthquakes, and wave action. The author conducted an extensive literature review of submarine slope failure events and found that among the 534 cataloged failures, earthquakes were directly responsible for more than 200 failures, making them the primary triggering mechanism. Marine waves were responsible for approximately 5% of the cataloged failures and are also an important cause of submarine slope failure. It's worth noting that these mechanisms can sometimes act in combination to cause instability. Most of stability analysis studies considered that wave action is the primary destabilizing loading component<sup>5–7</sup>. Few attention has been granted to the impact of combined wave and seismic actions on the stability conditions of a seabed. The present analysis shall specifically focus on evaluating the effects of gravity

Department of Civil Engineering, Federal University of Rio Grande do Sul, Porto Alegre, Brazil. ✉email: samir.maghous@ufrgs.br

waves propagating on the sea surface and seismic events, both of which being significant contributors to seabed instability.

As regards the poromechanical effects of waves on a submarine slope, it is first observed that surface waves induce orbital motions in water, which results in varying excess pore pressure distribution within the soil mass, particularly in the zones located under the wave crest and trough<sup>8,9</sup>. These pore pressure variations can potentially lead to offshore structure instability, as noted in previous studies<sup>10,11</sup>. A natural approach for addressing this issue would consist in computing the displacement and stress fields prevailing within the soil mass by solving an appropriate boundary value problem stated on the seabed material system. In that respect, one may quote the works by Madsen<sup>12</sup> and Yamamoto et al.<sup>13</sup> who formulated analytical solutions for the poroelastic response of a seabed in the context of linear wave theory and the work by Dormieux and Delage<sup>14</sup> extending this analysis to a more general form of wave loading. However, a more comprehensive investigation should incorporate nonlinear features of the soil constitutive behavior, such as the irreversible soil densification and associated pore pressure generation resulting from shear cyclic wave loading. The formulation of such nonlinear poromechanical behavior would rely upon field or laboratory evaluation of the constitutive parameters, which is generally not an easy task for marine soils, thus indicating that a yield design approach that requires only a few strength properties would reveal more suitable. As a consequence, insofar the assessment of seabed stability is the only objective, displacement-based approaches such as the incremental elastoplastic analysis until the free plastic flow of the structure is reached do not appear fully adequate, and the direct implementation of yield design or limit analysis theorems should be preferred. In that respect, two situations regarding the soil type should be distinguished when addressing the seabed stability issue.

Referring specifically to granular seabed soils, the pioneering works of Ishihara and Yamazaki<sup>15</sup> and Rahman and Jaber<sup>16</sup> have emphasized the crucial effect of pore pressure generation that is associated with soil densification under the shear cyclic wave loading. From the modeling viewpoint, the simplified methods formulated by these authors for evaluating the pore pressure induced in the seabed by the overpressure wave propagating along its surface have been significantly improved in Dormieux<sup>17</sup> and later in Dormieux et al.<sup>18</sup>.

Resorting to the theoretical framework of limit analysis and relates static and kinematic approaches<sup>19–21</sup>, the primary purpose of the present paper is to investigate the stability conditions of a seabed submitted to combined action of marine wave and seismic loading. Emphasis will be given to assess: (a) the destabilizing effects induced by seismic loading, and (b) the impact of seabed thickness on the seabed stability condition. Regarding the latter loading component, the pseudo-static method is used to account for the inertial forces developed in the seabed soil mass, presumably generated by the earthquake ground motion. This simplified approach has been widely used in geotechnical engineering to address the stability analysis of structures under seismic loading, the inertia forces associated with earthquake sequence being accounted for through equivalent static forces (e.g.<sup>22–25</sup>). It should be, however, emphasized that the material system collapse cannot be addressed through a simple comparison of the applied load, say  $Q$  for illustrative purpose, to the associated limit value  $Q^{\text{lim}}$  derived from pseudo-static analysis. Indeed, when  $Q^{\text{lim}}$  drops below  $Q$  at some time during the earthquake sequence, it does not necessarily imply a serious problem of the seabed<sup>22–25</sup>. What really matters is the magnitude of permanent displacements induced by the earthquake when  $Q^{\text{lim}}$  does lie below  $Q$ . If the accumulated displacement exceeds a certain limit, the system may be considered to have collapsed. This aspect of the stability analysis requires a dynamic analysis and cannot be addressed in the framework of the simplified pseudo-static method. At the material level, two situations shall be distinguished in the analysis according to the seabed constitutive material. For clayey or low permeability silty soils, the strength properties are described by a Tresca yield condition and the seabed stability analysis is carried out in the context of total stress analysis. Such a situation has been investigated under the static loading condition by Dormieux<sup>27</sup>, Dormieux<sup>17</sup>, Dormieux and Coussy<sup>28</sup> and Dormieux<sup>29</sup>, considering a seabed with infinite thickness subjected to wave loading. In the case of granular seabed soils for which the effect of pore pressure reveals fundamental, the soil strength capacities are modeled by means of a Mohr-Coulomb criterion expressed in terms of Terzaghi effective stress tensor. The seabed stability analysis is therefore developed in the framework of effective stress formulation of the limit analysis problem (see for instance<sup>17,18,30,31</sup>, to cite a few). In that case, the seepage forces associated with the gradient of excess pore pressure distribution should be previously evaluated and incorporated in the stability analysis problem. For this purpose, the present analysis extends the framework formulated in Dormieux et al.<sup>18</sup> to account for the effects of finite seabed layer and pseudo-static seismic forces in the seabed stability analysis.

## Statement of the stability problem

This section provides a description of the problem geometry as well as the loading mode in the static context. The formulation of the stability problem is then extended to account within a simplified framework for the loading induced by seismic forces.

## Geometry and loading mode in the static condition

The seabed is modeled as a half-space material domain  $\Omega$  whose upper boundary surface  $z = 0$  is inclined at an angle  $\theta \neq 0$  with respect to the horizontal plane (Fig. 1b). The inclination angle is assumed to be notably small:  $\theta \ll 1$ . The soil layer of thickness  $d$  is delimited at the top by the water-soil interface located at  $z = 0$ , where the positive axis points toward the sea surface, and at the bottom by a rigid and impermeable substrate located at  $z = -d$ . The particular case of a horizontal seabed where  $\theta = 0$  is also sketched in Fig. 1a.

In the absence of seismic inertial forces developed in the rock mass by the passage of seismic waves, the loading mode of the material system (the seabed) is the result of two types of forces: the body forces which apply in the soil mass and the surface forces acting along the upper boundary of the seabed. The body forces acting in the bed are the gravity forces  $\gamma \underline{e}_v = \rho g \underline{e}_v$  in which  $g$  is the gravity acceleration,  $\rho = \rho_s(1 - \varphi) + \rho_w \varphi$  is the average mass density of the porous medium,  $\varphi$  denotes the porosity which represents the fraction of the volume

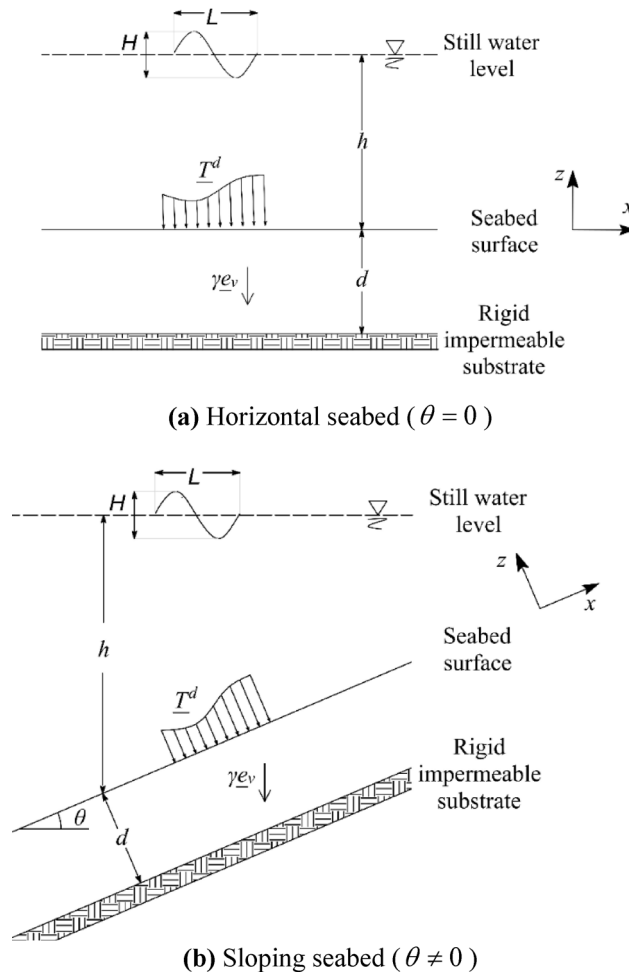


**Fig. 1.** Geometry of the seabed subjected to wave loading and gravity force in static condition.

occupied by the fluid;  $\rho_w$  and  $\rho_s$  denote the mass densities of the water and the solid, respectively, and  $\underline{e}_v$  stands for the downward unit vector:

$$\underline{e}_v = -\sin \theta \underline{e}_x - \cos \theta \underline{e}_z \tag{1}$$

In the context of the general description of plane wave loading, the surface forces  $\underline{T}^d$  acting on the boundary  $z = 0$  are defined by the hydrostatic pressure and the wave overpressure:

$$\underline{T}^d = T_s^d \underline{e}_z = -(p_{wave}(x, t) + \gamma_w h(x)) \underline{e}_z \text{ along } z = 0 \tag{2}$$

where  $\gamma_w = \rho_w g$  is the water unit weight and  $h = h(x)$  denotes the local water depth calculated from the horizontal still sea water level. It is observed that the value of  $h$  is constant for the horizontal plane seabed (Fig. 1a) whereas  $h(x) = h_0 - x \sin \theta$  decreases linearly with coordinate  $x$  in the case of sloping seabed (Fig. 1b),  $h_0$  being the water depth at the origin of  $x$ -axis. In the above expression, the term  $p_{wave}(x, t)$  refers to the overpressure induced by the wave at  $t$ . It should be emphasized that for usual seabed soils and wave velocity, the water wave velocity is generally small when compared to the soil shear wave velocity, thus suggesting that inertia effects associated with the water wave can be neglected<sup>28,32</sup>. It can therefore be considered that the wave loading acting on the seabed reduces to the overpressure  $p_{wave}(x, t)$ .

Regarding marine waves, water wave theories formulated in the context of hydrodynamics are generally classified into two major categories: small amplitude wave theories and long wave theories. The small amplitude wave theories embrace the linearized theory for infinitesimal amplitude waves and the first categories of power series, i.e., the power series in terms of  $H/L$  for finite amplitude waves. Long wave theories encompass numerical solution methods primarily used for nonlinear long wave Eq<sup>33</sup>. The linearized solution is obtained by finding a velocity potential function that satisfies the boundary conditions of the medium. This approach has proven to be extremely successful, even for the movement of waves with significant magnitude in shallow waters.

The wave loading is modeled by means of an overpressure  $p_{wave}(x, t)$  acting on the planar sea floor  $z = 0$ , with maximum amplitude  $p_0$ . In the context of first order (linear) Stokes theory, which is usually used in engineering practice, the expression of cyclic overpressure is given as<sup>34,35</sup>:

$$p_{wave}(x, t) = p_0 \sin \psi \text{ with } \psi = \lambda x - \omega t \quad (3)$$

where

$$p_0 = \frac{\gamma_w H/2}{\cosh \lambda h} \text{ with } \lambda = \frac{2\pi}{L} \text{ and } \omega = \frac{2\pi}{T} \quad (4)$$

where  $\lambda$  and  $\omega$  denote respectively the wave number and wave frequency,  $T$  is the wave period,  $H$  is the crest to trough height of the wave and  $L$  is the wave length. It should be recalled that expression of overpressure  $p_{wave}(x, t)$  is based on the assumption of irrotational flow of non-viscous and incompressible fluid over horizontal and impermeable seabed.

Waves originated in deep water ( $h > L/2$ ) travel towards the coast, occurring variation of its length, speed and height. It is assumed that the wave period is unchanged, regardless of the water depth. Referring to the wave parameters in deep water  $H_0$  and  $L_0$ , the values of the wave length  $L = L(h)$  and the wave crest to trough height wave  $H = H(h)$  at depth  $h$  are computed from the following expressions<sup>34</sup>:

$$L = L_0 \tanh 2\pi \frac{h}{L} \quad (5)$$

with

$$L_0 = \frac{gT^2}{2\pi} \quad (6)$$

$$H = H_0 \left\{ \left[ 1 + \frac{4\pi h/L}{\sinh(4\pi h/L)} \right] \tanh 2\pi \frac{h}{L} \right\}^{-1/2} \quad (7)$$

Expression (5) of  $L$  is obtained from the linear wave dispersion equation, whereas expression (7) of  $H$  is derived from energy conservation considerations.

The solution to the linearized Stokes wave problem is based on the free surface kinematic condition. In that respect, a further condition should be imposed on the wave characteristics for shallow water. Due to the phenomenon of wave-breaking, the set  $H$  of the triples  $(H, L, h)$  which are physically allowable is bounded. More precisely, the wave steepness  $H/L$  cannot increase beyond a certain critical value at which the wave breaks<sup>16,36</sup>:

$$H = \left\{ (H, L, h), \frac{H}{L} \leq \frac{1}{7} \tanh \left( \frac{2\pi h}{L} \right) \right\} \quad (8)$$

It should be kept in mind that above modeling of wave pressure assumes a horizontal sea floor, so that expressions (3) and (4) of wave overpressure represent a first approximation for the case of seabed with small inclination (i.e.,  $\theta \ll 1$ ). Moreover, although the linear wave theory assumes that the seabed is impermeable, it can be shown that the use of this theory is appropriate for granular beds, since the usual permeabilities of sediment do not significantly affect the overpressure induced by such a wave<sup>18</sup>. In addition, this theory can also be applied as a first approximation in the case of slightly inclined seabed<sup>28</sup>.

### Framework of pseudo-static method

The simplified framework that shall be used to account for earthquake-induced forces in the seabed stability analysis is briefly summarized in this section.

Stability analyses of earth slopes during earthquake shaking were first explored in the early twentieth century, employing what is now recognized as the pseudo-static method. The initial documented instance of pseudo-static method in technical literature was presented by Terzaghi in 1950. The pseudo-static method conceptualizes seismic shaking as a permanent body force integrated into the force-body diagram of a conventional static limit-equilibrium analysis<sup>23,37</sup>.

In most conventional engineering stability analyses, the concept of pseudo-static inertial forces, presumed to be generated by soil motion during seismic events, is classically adopted to assess the stability of soil masses using the Limit Analysis theory. Despite its limitations, the pseudo-static method is still widely used in geotechnical engineering because it has been proven effective and yields satisfactory results<sup>24</sup>. This analysis approach has been discussed in various works, such as those by Seed<sup>22</sup>, Saada et al.<sup>24</sup>, Belghali et al.<sup>25</sup> and Saada et al.<sup>26</sup>. The stability analysis developed in this paper relies upon the pseudo-static method, and dynamic effects of earthquake motions on the variations of the soil strength properties are disregarded.

The geometry of the problem is the same as that presented in the previous section, where the seabed is assumed to be a semi-infinite space with upper surface defined by the plan  $z = 0$  and inclined at an angle  $\theta$  with the horizontal. Under the assumption of plane strain conditions parallel to the plane  $xz$ , the configurations of horizontal plane seabed (Fig. 2a) and sloping seabed (Fig. 2b) are addressed in the analysis.

As regards the loading mode, the material system under consideration is basically submitted to the action of surface forces acting along the upper boundary of the seabed associated with the plane wave loading, as well as to gravity (soil unit weight  $\gamma$ ) and inertial forces developed in the soil layer by the passage of seismic waves. In the context of pseudo-static method, it useful to first introduce horizontal unit vector  $\underline{e}_h$  defined as (Fig. 2):

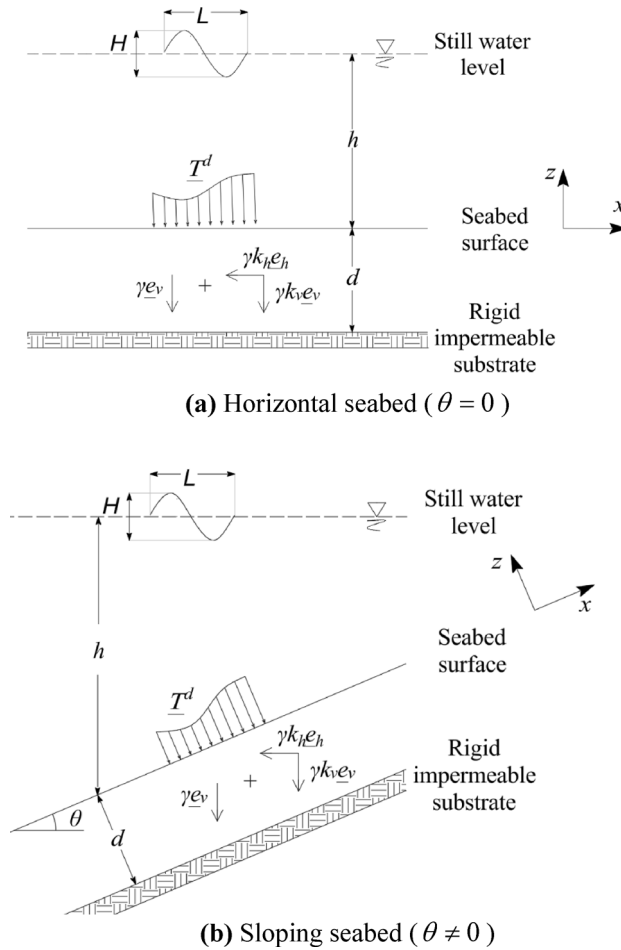


**Fig. 2.** Geometry and loading mode of the seabed within the framework of pseudo-static analysis.

$$e_h = -\cos \theta e_x + \sin \theta e_z \tag{9}$$

the vertical unit vector  $e_v$  being defined in Eq. (1). The first components of the loading are defined by the gravity forces  $\gamma e_v$  and their horizontal  $k_h \gamma e_h$  and vertical  $k_v \gamma e_v$  seismic acceleration counterparts, where  $k_h$  and  $k_v$  respectively denote the average horizontal and vertical seismic coefficients that stands in an approximate manner for the intensity of the distributed earthquake-induced inertia forces. These coefficients are generally correlated with the peak accelerations in typical seismic records. Referring, for instance, to the horizontal seismic coefficient, the value of  $k_h$  is evaluated in most international standards as a fraction, generally ranging from 0.3 to 0.5, of the ratio  $\bar{a}_{\max}/g^{38}$ , where  $\bar{a}_{\max}$  is the average of peak horizontal acceleration values recorded over the characteristic time duration of the earthquake.

From a theoretical viewpoint, the surface forces acting along the upper boundary at  $z = 0$  would consist of two components: surface forces due to wave overpressure and hydrostatic pressure under static condition  $T_s^d = T_s^d e_z$  defined in Eq. (2) as well as pseudo-static counterpart surface forces  $T_a^d = k_h (T_s^d \cdot e_h) e_h + k_v (T_s^d \cdot e_v) e_v$  evaluated from the static component and the seismic coefficients  $k_h$  and  $k_v$ . However, application of such pseudo-static surface load will induce shear stresses along the ground surface, which is not commonly considered in the pseudo-static stability analyses involving external water pressure forces. In that respect, the following simplified framework will be adopted throughout the subsequent stability analysis for the loading model:

- The forces acting on the seabed surface  $z = 0$  reduce to the static distribution  $T_s^d e_z$ , thus disregarding the contribution of pseudo-static load component  $T_a^d$ :

$$T^d \approx T_s^d e_z \text{ along } z = 0 \tag{10}$$

in which  $T_s^d = -p(x, t)$ . It is observed that the above assumption amounts to underestimating the surface loading, thus leading to unconservative approach from an engineering design viewpoint.

The value of fluid pressure at the sea floor  $p(x, t) = p_{wave}(x, t) + \gamma_w h(x)$  acting along the seabed boundary  $z = 0$  is not affected by the passage of earthquake waves. In particular, expression of  $p_{wave}$  is still defined by Eqs. (3) and (4). It should be however pointed out that ground seismic shaking during earthquake sequences

can affect the hydrodynamic wave-induced pressure (e.g.<sup>39–43</sup>). Nevertheless, a recent study by Yu et al.<sup>44</sup> indicated that the combined wave and earthquake effects do not lead to a significant amplification of the near-bed hydrodynamic pressure, thus suggesting that its fluctuations may reasonably be neglected in the stability analysis. A comprehensive modeling of the wave-earthquake interaction and its impact on seabed stability would require a dynamic response analysis that incorporate the whole acceleration time history and associated wave-induced pressure fluctuations, which falls beyond the scope of the present pseudo-static analysis.

The formulation of stability analysis problem within the framework of limit analysis theory requires to previously define introducing the strength capacity of the saturated porous material. The latter is expressed under a general yield condition form  $f(\underline{\sigma}, p) \leq 0$ , where  $\underline{\sigma}$  and  $p$  denote respectively the stress and pore pressure fields in the porous seabed medium. For a given time  $t$  within the time interval considered for the study, the stability condition of the seabed structure under applied loading mode stems from compatibility between the equilibrium of the considered seabed structure and the resistance of its constituent porous material:

$$\text{Stability} \Leftrightarrow \exists \underline{\sigma} \text{ such that } \begin{cases} \text{div} \underline{\sigma} + \gamma \underline{e}_v + \gamma \underline{e}_a = 0 & \text{in } \Omega \\ \underline{T} = \underline{T}^d & \text{along } z = 0 \\ f(\underline{\sigma}, p) \leq 0 & \text{in } \Omega \end{cases} \quad (11)$$

in which vector  $\underline{e}_a$  is given by:

$$\underline{e}_a = k_h \underline{e}_h + k_v \underline{e}_v \quad (12)$$

and  $\underline{T} = \underline{\sigma} \cdot \underline{e}_z$  is the stress vector acting upon the upper surface of the seabed, while the prescribed surface load  $\underline{T}^d$  is given by Eq. (10).

The case of stability analysis under static condition is retrieved by setting  $k_v = k_h = 0$  in the above stability condition (12), leading to  $\underline{e}_a = 0$  and  $\underline{T}^d = T_s^d \underline{e}_z$ :

$$\text{Stability} \Leftrightarrow \exists \underline{\sigma} \text{ such that } \begin{cases} \text{div} \underline{\sigma} + \gamma \underline{e}_v = 0 & \text{in } \Omega \\ \underline{T} = \underline{T}^d & \text{along } z = 0 \\ f(\underline{\sigma}, p) \leq 0 & \text{in } \Omega \end{cases} \quad (13)$$

The stability problem (11) may be conveniently addressed by introducing the set  $K$  of safe loads  $\underline{Q} = (\gamma (\underline{e}_v + \underline{e}_a), \underline{T}^d)$ , as introduced in the limit analysis theory<sup>21</sup>. The convex domain  $K$ , also referred to as the stability domain, is defined by the loads  $\underline{Q}$  equilibrated by stress distributions that comply at any point of the seabed with the strength condition:

$$K = \{ \underline{Q}; \exists \underline{\sigma} \text{ statically admissible with } \underline{Q} \text{ and } \forall \underline{x} \in \Omega f(\underline{\sigma}, p) \leq 0 \} \quad (14)$$

Before further developments, it should be emphasized that the dynamic effects of earthquake sequences on the porous medium strength properties, such as cyclic shear strength degradation, cannot be accounted for in the context of the present simplified pseudo-static analysis.

### Stability analysis of a purely cohesive seabed soil – total stress analysis

In the context of total stress stability analysis, the strength capacities of the porous soil mass are classically described by a purely cohesive Tresca-like failure condition. In such an approach, the pore pressure distribution is assumed not to explicitly control the yield failure of the material, i.e.,  $f(\underline{\sigma}, p) = f(\underline{\sigma})$ . In the present analysis, the material strength criterion is defined by a non-homogeneous Tresca criterion in which the cohesion  $C(z)$  increases linearly with the distance to the boundary  $z = 0$ :

$$f(\underline{\sigma}, z) = \sup(\sigma_i - \sigma_j) - 2C(z) \leq 0 \text{ with } C(z) = \eta|z| \quad (15)$$

where  $\sigma_i$ , with  $i \in \{1, 2, 3\}$  stand for the principal stresses of total stress tensor  $\underline{\sigma}$ . The scalar  $\eta$ , referred to as the cohesion gradient, is the single constitutive parameter required in this analysis. From a practical standpoint, the cohesion gradient of marine soil can be estimated from field tests such as Cone Penetration Testing (CPT), with reference values typically close to  $\eta = 1.4 \text{ kPa/m}^{45}$ . Convention of positive stress in tensile is adopted throughout the paper. It should be emphasized that such a failure condition is suitable for modeling the strength capacities of clayey or low permeability silty soils under undrained loading conditions, for which a total stress analysis proves relevant. The above purely cohesive yield criterion is notably well adapted to the case of normally consolidated sedimentary clays, which constitute a substantial part of the ocean floor. The reasoning developed for seabed stability is carried out in the context of total stress analysis according to the formulation defined in Eq. (11) together with failure condition (15). The stability problem has been originally handled in Dormieux and Coussy<sup>28</sup> considering static loading condition ( $k_v = k_h = 0$ ) and infinite seabed layer thickness ( $d \rightarrow +\infty$ ). In that respect, the present stability analysis extends the previous results obtained in Dormieux and Coussy<sup>28</sup> to the configuration of a seabed of finite thickness with consideration of seismic loading.

It should be observed that the stress fields investigated in the stability analysis comply with the assumption of plane strains parallel to  $xz$ -axes, that is,

$$\underline{\sigma}(x, z) = \sigma_{xx} \underline{e}_x \otimes \underline{e}_x + \sigma_{zz} \underline{e}_y \otimes \underline{e}_y + \sigma_{xz} (\underline{e}_x \otimes \underline{e}_z + \underline{e}_z \otimes \underline{e}_x) + \sigma_{yy} \underline{e}_y \otimes \underline{e}_y \quad (16)$$

where the dependence of  $\underline{\sigma}$  with respect to time has been omitted for the sake of simplicity. In the framework of plane strain stability analysis problem (11), the 'plane strain' strength criterion of the constitutive material can be equivalently written as follows:

$$f(\underline{\sigma}, z) = \sqrt{(\sigma_{xx} - \sigma_{zz})^2 + 4\sigma_{xz}^2} - 2C(z) \leq 0 \quad (17)$$

which depends only on the in-plane stress components  $(\sigma_{xx}, \sigma_{zz}, \sigma_{xz})$ . A rigorous formulation of the yield design theory in the context of plane strain condition may be found in Salençon<sup>19</sup>. In particular, the yield condition (17) expressing the strength capacities under plane strain condition is deduced from the three-dimensional Tresca yield criterion (15) by minimization with respect to the value of principal stress along the  $y$ -axis. In this framework, the stability problem handled in the subsequent analysis will therefore be developed in the two-dimensional matrix formalism in which a generic stress field is represented by its in-plane components:

$$\underline{\sigma} = \begin{bmatrix} \sigma_{xx} & \sigma_{xz} \\ \sigma_{zx} & \sigma_{zz} \end{bmatrix} \quad \text{with } \sigma_{zx} = \sigma_{xz} \quad (18)$$

One can notice that there are no restrictions on the soil layer thickness in the formulation employed.

### Lower bound static approach

In this section, the seabed stability problem is investigated by means of the yield design static approach, which consists of the direct implementation of stability definition (11) through the exhibition of a stress field that is statically admissible in the loading mode and complying with the strength condition (17). For this purpose, the basic idea is to split the loading applied to seabed into four elementary components and then to formulate for each loading component an associated statically admissible stress field. More precisely,

- The two first components of the loading are the gravity forces  $\gamma e_v$  and the hydrostatic pressure  $\gamma_w h(x)$  acting along the seabed surface (It is recalled that the local water depth is  $h(x) = h_0 - x \sin \theta$ ). The stress fields associated by the equilibrium conditions are respectively defined as:

$$\underline{\sigma}^g = \gamma z \begin{bmatrix} \cos \theta & \sin \theta \\ \sin \theta & \cos \theta \end{bmatrix} \underline{\sigma}^{hyd} = -\gamma_w \begin{bmatrix} h(x) & z \sin \theta \\ z \sin \theta & h(x) \end{bmatrix} \quad (19)$$

It is readily seen that  $\text{div} \underline{\sigma}^g + \gamma e_v = 0$  and  $\text{div} \underline{\sigma}^{hyd} = 0$ , whereas the corresponding stress vectors acting upon the boundary  $z = 0$  comply with  $\underline{\sigma}^g \cdot e_z = 0$  and  $\underline{\sigma}^{hyd} \cdot e_z = -\gamma_w h(x) e_z$ .

- The third loading component is the wave overpressure  $p_{wave}(x, t) = p_0 \sin \psi$  defined by (3) in the context of linear theory. It is first observed that for two different times  $t$  and  $t'$ ,  $p_{wave}(x, t)$  and  $p_{wave}(x, t')$  are simply deduced from each other by translation parallel to  $x$ -axis. Since the strength criterion defined in (15) or (17) is independent of coordinate  $x$ , the stability problem under overpressure  $p_{wave}(x, t)$  is therefore of time independent of  $t$ . Accordingly, the stability analysis can be developed considering  $t = 0$  without loss of generality. Reference to time  $t$  will therefore be omitted and the corresponding overpressure is then defined by  $p_{wave}(x) = p_0 \sin \lambda x$ . In order to obtain a stress field statically admissible with applied wave overpressure, the idea consists in considering the stress field prevailing in an elastic half space submitted to an arbitrary pressure distribution. The latter stress solution, denoted by  $\underline{\sigma}^{p_{wave}}$ , has been formulated in Dormieux and Delage<sup>14</sup> and Dormieux and Coussy<sup>28</sup>. It takes the following form:

$$\sigma_{xx}^{p_{wave}} = -u - z \frac{\partial u}{\partial z}; \quad \sigma_{zz}^{p_{wave}} = -u + z \frac{\partial u}{\partial z}; \quad \sigma_{xz}^{p_{wave}} = \sigma_{zx}^{p_{wave}} = z \frac{\partial u}{\partial x} \quad (20)$$

where function  $(x, z) \in \mathbb{R} \times \mathbb{R}^- \rightarrow u(x, z)$  satisfy the following conditions:

$$\begin{cases} \Delta u = 0 & \forall (x, z) \in \mathbb{R} \times \mathbb{R}^- \\ u(x, z = 0) = p_{wave}(x) & \forall x \in \mathbb{R} \end{cases} \quad (21)$$

in which  $\Delta$  stands for the Laplacian operator. The static admissibility of  $\underline{\sigma}^{p_{wave}}$  with the wave overpressure loading can be readily verified, that is,  $\text{div} \underline{\sigma}^{p_{wave}} = 0$  and  $\underline{\sigma}^{p_{wave}} \cdot e_z = -p_{wave}(x) e_z$  along the boundary  $z = 0$ .

Based on the property that the wave overpressure  $x \rightarrow p_{wave}(x)$  is a continuous and bounded function, Dormieux and Coussy<sup>28</sup> showed that the following integral defines a particular solution to problem (21):

$$u(x, z) = \frac{p_0}{\pi} \int_{-\infty}^{+\infty} \sin \lambda(x + \vartheta z) \frac{d\vartheta}{1 + \vartheta^2} = p_0 e^{\lambda z} \sin \lambda x \quad (22)$$

The stress field considered for the lower static approach can therefore be defined as

$$\underline{\underline{\sigma}}^{pwave} = p_0 e^{\lambda z} \begin{bmatrix} -(1 + \lambda z) \sin \lambda x & \lambda z \cos \lambda x \\ \lambda z \cos \lambda x & -(1 - \lambda z) \sin \lambda x \end{bmatrix} \quad (23)$$

- The final component of the stress field, statically consistent with the loading due to the pseudo-static body forces  $\gamma e_a$ , is given by:

$$\underline{\underline{\sigma}}_a^g = \gamma z \begin{bmatrix} -k_1 & k_2 \\ k_2 & k_1 \end{bmatrix} \quad (24)$$

where parameters  $k_1$  and  $k_2$  are defined from the seismic coefficients by:

$$k_1 = -k_h \sin \theta + k_v \cos \theta, \quad k_2 = k_h \cos \theta + k_v \sin \theta \quad (25)$$

The above stress fields are statically admissible with the corresponding seismic loading since they comply with the following conditions:

$$\operatorname{div} \underline{\underline{\sigma}}_a^g + \gamma e_a = 0 \text{ and } \underline{\underline{\sigma}}_a^g \cdot \underline{n} = 0 \text{ along } z = 0 \quad (26)$$

Combining the above four elementary stress fields, the static approach is then formulated considering the following stress field:

$$\underline{\underline{\sigma}} = \underline{\underline{\sigma}}^g + \underline{\underline{\sigma}}^{hyd} + \underline{\underline{\sigma}}^{pwave} + \underline{\underline{\sigma}}_a^g \quad (27)$$

which is statically admissible in the loading mode. In order to be compatible with soil strength capacities, the stress field thus defined by Eq. (27) must satisfy the yield condition (17) at any point  $(x, z) \in \mathbb{R} \times \mathbb{R}^-$ , that is

$$\max_{\mathbb{R} \times \mathbb{R}^-} \sqrt{(\sigma_{xx} - \sigma_{zz})^2 + 4\sigma_{xz}^2} - 2C(z) \leq 0 \quad (28)$$

Thus, by substituting Eqs. (19), (23) and (24) into (27), and then replacing (17) and (27) into condition (28), one can write:

$$\left\{ (\lambda p_0 e^{\lambda z} \sin \lambda x + \gamma k_1)^2 + (\gamma' \sin \theta + \lambda p_0 e^{\lambda z} \cos \lambda x + \gamma k_2)^2 \right\}^{1/2} \leq \eta \quad \forall x \in \mathbb{R}, \forall z \leq 0 \quad (29)$$

in which  $\gamma' = \gamma - \gamma_w$ .

The most restrictive condition is obtained by means of maximization of the left-hand side of above sufficient stability condition (29). From a strictly mathematical viewpoint, two situations should be distinguished for this purpose:

- $\gamma' \sin \theta + \gamma k_2 = 0$

In that particular case, which implies  $\theta = 0$  and  $k_2 = 0$ , it can be readily established from the maximization procedure that the most restrictive condition reads

$$\lambda p_0 + \gamma k_1 \leq \eta \quad (30)$$

- $\gamma' \sin \theta + \gamma k_2 \neq 0$

It stems from the analysis of maximization problem that the most restrictive condition is achieved for  $x = x^*$  and  $z = 0$ , with

$$\tan \lambda x^* = \frac{\gamma k_1}{\gamma' \sin \theta + \gamma k_2} \quad (31)$$

yielding the following sufficient stability condition:

$$\lambda p_0 + \sqrt{(\gamma' \sin \theta + \gamma k_2)^2 + (\gamma k_1)^2} \leq \eta \quad (32)$$

It is observed that condition (30) is actually retrieved from (32) as a particular case by simply setting  $\gamma' \sin \theta + \gamma k_2 = 0$ , so that inequality (32) represents a general sufficient stability condition. In other words, it defines the set of loading parameters for which the seabed stability is ensured. It is also emphasized that the static approach will effectively provide non-trivial lower bound solution for the seabed stability as soon as the following condition is fulfilled:

$$\eta_s = \sqrt{(\gamma' \sin \theta + \gamma k_2)^2 + (\gamma k_1)^2} \leq \eta \tag{33}$$

which can be interpreted as a sufficient condition for the stability of the seabed in the absence of wave overpressure (i.e.  $p_0 = 0$ ), that is, under the combined action of gravitational forces, hydrostatic pressure, and pseudo-static forces ( $\gamma k_1, \gamma k_2$ ). However, a simple comparison analysis shows that (32) is a more restrictive condition than condition (33).

The stability criterion (32) obtained from the static limit analysis provides a lower bound approach to the convex domain  $K$  of allowable loads introduced in (14):

$$K^s = \left\{ \underline{Q}; \quad \lambda p_0 - \eta + \sqrt{(\gamma' \sin \theta + \gamma k_2)^2 + (\gamma k_1)^2} \leq 0 \right\} \subseteq K \tag{34}$$

It is worth noting that the proposed static approach to domain  $K$  leads to a sufficient condition for seabed stability that is independent of the soil layer thickness  $d$ .

### Upper bound kinematic approach

The upper bound approach to stability convex  $K$  is based on the implementation of two piecewise translational failure mechanisms. For a given point  $M$  located on the seabed surface  $z = 0$ , two virtual velocity fields depicted in Fig. 3a ( $\theta = 0$ ) and in Fig. 3b ( $\theta \neq 0$ ) are examined. The two triangular blocks  $MM'A$  and  $MM'B$  are endowed with translational motions respectively parallel to the directions of  $M'A$  and  $M'B$ :

$$\underline{U}(MM'A) = -\varepsilon U(\cos \alpha \underline{e}_x + \sin \alpha \underline{e}_z) \quad \underline{U}(MM'B) = \varepsilon U(-\cos \alpha \underline{e}_x + \sin \alpha \underline{e}_z) \tag{35}$$

where  $U > 0$  is a translation velocity magnitude positive scalar and  $\varepsilon = \pm 1$ . The remaining part of seabed ground is kept motionless. The geometry of the considered failure mechanisms is defined by the abscissa  $a$  of point  $M$  along the boundary surface  $z = 0$ , the length  $l$  of segments  $MA$  and  $MB$  (i.e.,  $l = MA = MB$ ) and the angle  $\underline{U}$ .

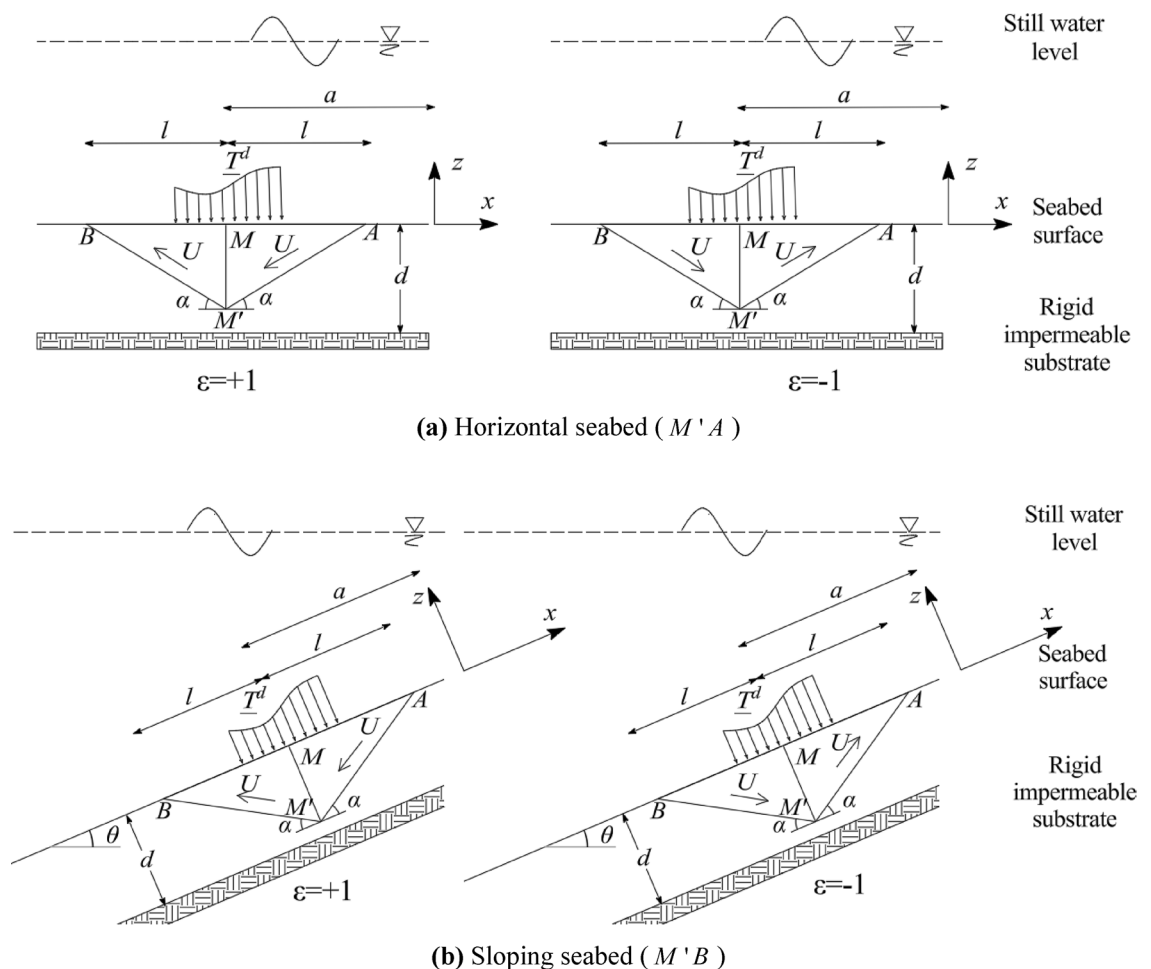


Fig. 3. Piecewise translational velocity fields  $\underline{U}$ .

The considered failure mechanisms involve velocity discontinuity along the lines  $M'A$  and  $M'B$ . Reflecting the normality rule for the Tresca soil failure condition (15), the velocity jump  $\underline{W}$  between the blocks  $MM'A$  and  $MM'B$  is oriented parallel to the line  $MM'$ :

$$\underline{W} = 2\varepsilon U \sin \alpha \underline{e}_z \tag{36}$$

The kinematic theorem of limit analysis states the following necessary stability condition of the seabed material system under applied loading:

$$P_{ext}(\underline{U}) \leq P_{mr}(\underline{U}) \tag{37}$$

which simply expresses in dual form the compatibility between the structure equilibrium equations and the soil strength requirement expressed by the yield condition. In the above inequality,  $P_{ext}(\underline{U})$  refers to the rate of work performed by the external loads, whereas the term  $P_{mr}(\underline{U})$  stands for the maximum rate of resisting work developed in the considered velocity field  $\underline{U}$ . The necessary stability condition (37) should be satisfied for any values of the geometrical parameters  $\alpha \in ]0, \pi/2[$ ,  $l \geq 0$  and  $\varepsilon = \pm 1$  defining the failure mechanisms.

The rate of external work  $P_{ext}(\underline{U})$  includes the contributions of gravity forces  $P_\gamma$ , the hydrostatic pressure  $P_{hyd}$ , the wave overpressure  $P_{wave}$  and the seismic components associated with gravity forces  $P_\gamma^s$ :

$$P_{ext}(\underline{U}) = P_\gamma + P_{hyd} + P_{wave} + P_\gamma^s \tag{38}$$

The contribution  $P_\gamma$  of the gravity forces to the rate of external work is computed as:

$$P_\gamma = \int_{\Omega} \gamma \underline{e}_v \cdot \underline{U} \, d\Omega = \varepsilon U \gamma l^2 \sin \alpha \sin \theta \tag{39}$$

where  $\Omega$  refers to blocks  $MM'A$  and  $MM'B$ . The contributions of hydrostatic pressure and wave overpressure to the rate of external work respectively read

$$P_{wave} = \int_{AB} -p_{wave} \underline{e}_z \cdot \underline{U}(x, 0) \, dx = \frac{2\varepsilon U p_0}{\lambda} \sin \alpha \cos \lambda a (1 - \cos \lambda l) \tag{40}$$

and

$$P_{hyd} = \int_{AB} -\gamma_w h(x) \underline{e}_z \cdot \underline{U}(x, 0) \, dx = -\varepsilon U \gamma_w l^2 \sin \theta \sin \alpha \tag{41}$$

The rate of work  $P_\gamma^s$  developed by the pseudo-static forces expresses as

$$P_\gamma^s = \int_{\Omega} \gamma \underline{e}_a \cdot \underline{U} \, d\Omega = \varepsilon U k_2 \gamma l^2 \sin \alpha \tag{42}$$

Introducing Expressions (39)-(42) into (38) yields

$$P_{ext}(\underline{U}) = \varepsilon U \left\{ \gamma l^2 \sin \alpha (\sin \theta + k_2) - \gamma_w l^2 \sin \theta \sin \alpha + \frac{2p_0}{\lambda} \sin \alpha \cos \lambda a (1 - \cos \lambda l) \right\} \tag{43}$$

Denoting by  $[\underline{U}]$  the velocity jump along the velocity discontinuity lines  $\Sigma = M'A \cup M'B \cup M'M$ , the maximum rate of resisting work  $P_{mr}(\underline{U})$  developed in the considered failure mechanisms is computed from the support function  $\Pi([\underline{U}])$  related to velocity jump and associated with the Tresca yield condition (15)<sup>21</sup>:

$$\Pi([\underline{U}]) = C(z) |[\underline{U}]| = \begin{cases} C(z) U & \text{along } M'A \text{ and } M'B \\ C(z) |\underline{W}| = 2C(z) U \sin \alpha & \text{along } MM' \end{cases} \tag{44}$$

Hence,

$$P_{mr}(\underline{U}) = \int_{\Sigma} \Pi([\underline{U}]) \, ds = U \left\{ \int_{M'A} C(z) \, ds + \int_{M'B} C(z) \, ds + 2 \sin \alpha \int_{M'M} C(z) \, ds \right\} \tag{45}$$

Recalling that the soil cohesion is defined by the linear function  $C(z) = \eta |z|$ , one obtains:

$$P_{mr}(\underline{U}) = \eta l^2 U \sin \alpha \frac{1 + \sin^2 \alpha}{\cos^2 \alpha} \tag{46}$$

Applying the kinematic inequality (37) with expressions (44) and (46) to compute  $P_{ext}(\underline{U})$  and  $P_{mr}(\underline{U})$  yields the following condition:

$$\varepsilon \left\{ \gamma' \sin \theta + \gamma k_2 + \frac{2p_0}{\lambda l^2} [\cos \lambda a (1 - \cos \lambda l)] \right\} \leq \eta \frac{1 + \sin^2 \alpha}{\cos^2 \alpha} \quad \forall l \geq 0, \forall \alpha \in ]0, \pi/2[ \tag{47}$$

Minimization with respect to angular parameter  $\alpha$  shows that the most restrictive condition corresponds to  $\alpha \rightarrow 0$ :

$$\left| \gamma' \sin \theta + \gamma k_2 + \frac{2p_0}{\lambda l^2} [\cos \lambda a(1 - \cos \lambda l)] \right| \leq \eta \quad \forall l \geq 0 \tag{48}$$

The best upper bound approach derived from considered failure mechanisms is obtained by maximizing the left-hand side of the inequality (48) with respect to geometrical parameters  $l$  and  $a$ . It is readily found that the optimal values of these parameters are given by  $l \rightarrow 0$  and  $a \rightarrow 0$ , which define a vanishing critical failure mechanism. As previously observed in Dormieux<sup>17</sup>, this particular characteristic of the optimal failure mechanism is mainly attributed to vanishing soil cohesion at the seabed surface  $C(0) = 0$ . Accordingly, the necessary condition for seabed stability is expressed by the following inequality:

$$\lambda p_0 + \gamma' \sin \theta + \gamma k_2 \leq \eta \tag{49}$$

In the absence of wave overpressure, i.e.  $p_0 = 0$ , the above condition reduces to

$$\eta_c = \gamma' \sin \theta + \gamma k_2 \leq \eta \tag{50}$$

which can be interpreted as a necessary condition for the seabed stability of the seabed under combined action of gravity forces, hydrostatic pressure and pseudo-static forces.

The stability condition (49) derived from the implementation of kinematic approach provides an upper bound estimate for the stability convex  $K$ :

$$K^c = \left\{ \underline{Q}; \quad \lambda p_0 - \eta + \gamma' \sin \theta + \gamma k_2 \leq 0 \right\} \supseteq K \tag{51}$$

### Conjunction of lower and upper bound approaches

The limit analysis reasoning based on static lower bound (32) and kinematic upper bound (49) conditions allows bracketing the domain of allowable loads applied to the seabed. For a fixed set of seismic coefficients  $k_h$  and  $k_v$ , it may be convenient for the graphical representation to characterize the loading mode by means of two components  $\underline{Q} = (Q_1 = \lambda p_0, Q_2 = \gamma')$ . In this context, three situations should be distinguished according to sufficient and necessary stability conditions (33) and (50) obtained in the absence of wave overpressure:

- If  $\eta \leq \eta_c$ , the necessary condition (50) indicates that the seabed is unconditionally instable.
- For  $\eta_c \leq \eta < \eta_s$ , the sufficient condition (32) together with (50) indicate that the proposed static approach does not provide an effective lower bound estimate for allowable loads. The approaches to convex  $K$  developed in the preceding sections actually reduce to the upper bound estimate  $K \subseteq K^c$ . Referring to the plane  $(Q_1, Q_2)$ , the triangular domain  $K^c$  is depicted Fig. 4a:

$$K^c = \{(Q_1, Q_2); \quad Q_1 + Q_2(\sin \theta + k_2) \leq \eta - \gamma_w k_2\} \tag{52}$$

It is observed that condition  $\eta_c \leq \eta$  implies the limit values  $Q_1^+ = \eta - \gamma_w k_2$  and  $Q_2^+ = \frac{\eta - \gamma_w k_2}{\sin \theta + k_2}$  are always positive.

- If  $\eta_s \leq \eta$ , both static and kinematic approaches lead to non-trivial estimates of convex  $K$ . As illustrated in Fig. 4b, the latter is bounded in the plane  $(Q_1, Q_2)$  from inside by the triangular domain  $K^s$  and from outside by the triangular domain  $K^c$ . Domain  $K^c$  is still defined by (52), whereas domain  $K^s$  is described by:

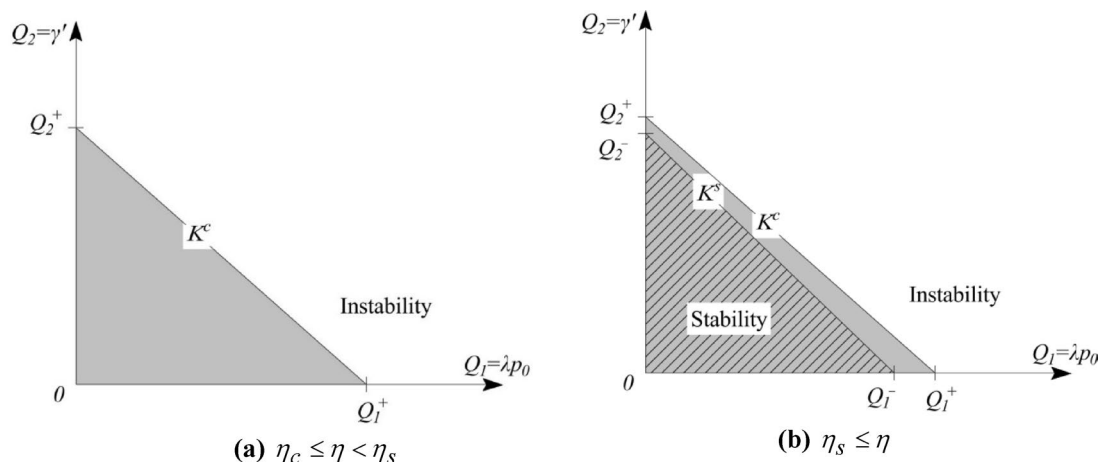


Fig. 4. Schematic representation of domains  $K^s \subseteq K \subseteq K^c$  in the plane  $(Q_1, Q_2)$ .

$$K^s = \left\{ (Q_1, Q_2) ; Q_1 + \sqrt{(Q_2(\sin \theta + k_2) + \gamma_w k_2)^2 + ((Q_2 + \gamma_w)k_1)^2} \geq \eta \right\} \tag{53}$$

Referring to the notations of Fig. 4b, the limit loads  $Q_1^- \geq 0$  and  $Q_2^- \geq 0$  are defined as

$$Q_1^- = \eta - \gamma_w \sqrt{k_2^2 + k_1^2} \quad , \quad Q_2^- = \frac{-\gamma_w [k_2(\sin \theta + k_2) + k_1^2] + \sqrt{\Delta}}{(\sin \theta + k_2)^2 + k_1^2} \tag{54}$$

with  $\Delta = \gamma_w^2 (k_2(\sin \theta + k_2) + k_1^2) + (\eta^2 - \gamma_w^2(k_1^2 + k_2^2)) ((\sin \theta + k_2)^2 + k_1^2)$ . It can readily be verified that condition  $\eta_s \leq \eta$  implies that scalar  $\Delta$  is always positive.

Keeping in mind the assumption  $\theta \ll 1$  for the seabed inclination and observing that the effect of vertical seismic coefficient is neglected in most practical applications, it appears that the value of coefficient  $k_1$  will generally be very small when compared to  $k_2$ , thus leading to approximation  $Q_1^+ \approx Q_1^- = \eta - \gamma_w k_2$ .

For the sake of conciseness, condition  $\eta_s \leq \eta$  will be assumed throughout the subsequent developments.

When the loading components ( $\gamma, \gamma_w$ ) and seismic coefficients ( $k_h, k_v$ ) are viewed as prescribed parameters, the seabed stability can alternatively be characterized by evaluating the limit value  $p_0^{lim}$  of wave overpressure. The lower and upper bounds of the latter are straightforwardly deduced from inequalities (32) and (49):

$$\frac{\eta - \sqrt{(\gamma' \sin \theta + \gamma k_2)^2 + (\gamma k_1)^2}}{\lambda} \leq p_0^{lim} \leq \frac{\eta - \gamma' \sin \theta - \gamma k_2}{\lambda} \tag{55}$$

Most design standards recommend the use of value  $k_v = 0$  in stability analyses, which amounts to considering only the horizontal seismic coefficient  $k_h$ <sup>23,46</sup>. Within this framework, the above inequalities thus simplify to:

$$\frac{\eta - \sqrt{(\gamma' \sin \theta + \gamma k_h \cos \theta)^2 + (-\gamma k_h \sin \theta)^2}}{\lambda} \leq p_0^{lim} \leq \frac{\eta - \gamma' \sin \theta - \gamma k_h \cos \theta}{\lambda} \tag{56}$$

which lead to coincident lower and upper bounds in the case of horizontal seabed (i.e.  $\theta = 0$ ):

$$p_0^{lim} = \frac{\eta - \gamma k_h}{\lambda} \tag{57}$$

Under the static conditions defined by  $k_v = k_h = k_1 = k_2 = 0$ , the lower and upper bound domains respectively defined by (34) and (51) are coincident. The convex  $K$  of allowable loads is therefore determined as

$$K = \{ Q = (Q_1 = \lambda p_0, Q_2 = \gamma') \quad ; \quad Q_1 \leq \eta - Q_2 \sin \theta \} \tag{58}$$

Fig. 5 provides a geometrical representation (hatched area) of domain  $k$  in the plane ( $Q_1, Q_2$ ).

As regards the limit value  $p_0^{lim}$  of wave overpressure, it follows from (56) that

$$p_0^{lim} = \frac{\eta - \gamma' \sin \theta}{\lambda} \tag{59}$$

which is identical to the result presented in Dormieux and Coussy<sup>28</sup> and Madalozzo<sup>47</sup>. The above result indicates that the effect of seabed inclination  $\theta \neq 0$  is formally equivalent to a reduction in the soil cohesion gradient by an amount equal to  $\gamma' \sin \theta$ .

Prior to further developments, it is important to emphasize that the stability conditions derived from the present static and kinematic approaches revealed independent of the soil layer thickness  $d$ .

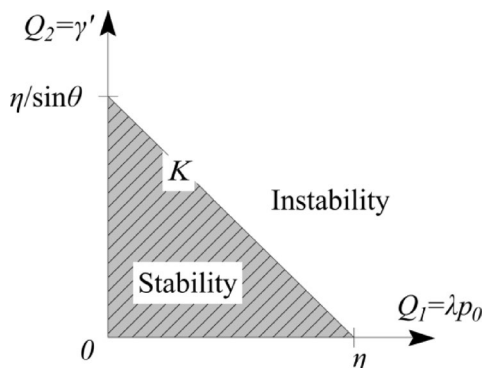


Fig. 5. Figure 5 Geometrical representation of stability domain  $K$  obtained under static conditions.

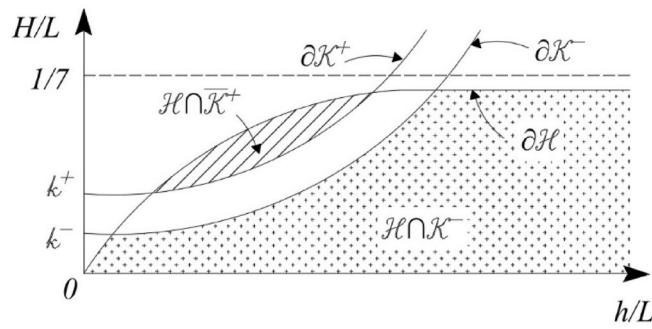


Fig. 6. Domain defining allowable linear waves in the plane  $(H/L, h/L)$ .

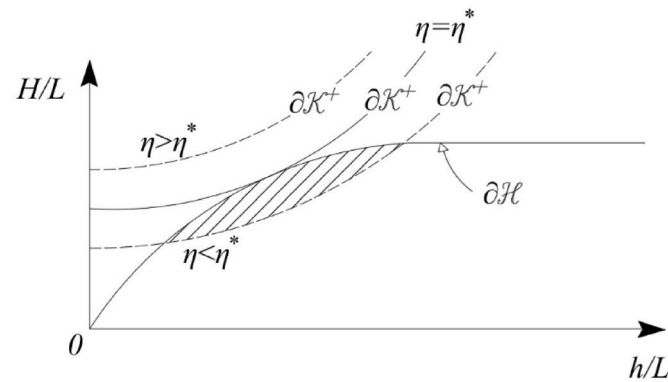


Fig. 7. Stability conditions in terms of the critical cohesion gradient  $\eta^*$ .

**Stability conditions in term of the linear wave parameters**

Instead of expressing the seabed stability in terms of conditions on the wave overpressure regarded as loading parameter, it is convenient for practical applications to characterize the set  $K$  of wave parameters  $(H, L, h)$  for which stability is ensured. It follows from expressions (4) defining the wave overpressure amplitude together with static and kinematic approaches (34) and (52):

$$K^- \subseteq K \subseteq K^+ \quad \text{with} \quad \begin{aligned} K^- &= \left\{ (H, L, h), \frac{H}{L} \leq \frac{\eta - \eta_s}{\pi \gamma_w} \cosh 2\pi \frac{h}{L} \right\} \\ K^+ &= \left\{ (H, L, h), \frac{H}{L} \leq \frac{\eta - \eta_c}{\pi \gamma_w} \cosh 2\pi \frac{h}{L} \right\} \end{aligned} \quad (60)$$

Clearly enough, the above definition considers that the remaining loading components  $(\gamma, \gamma_w)$  and seismic coefficients  $(k_h, k_v)$  are fixed parameters, since  $\eta_s$  and  $\eta_c$  depend of these parameters.

Referring to the plane  $(h/L, H/L)$ , the lower and upper bound estimates of the set  $K$  are plotted in Fig. 6. In this reference plane, the domain boundaries  $\partial K^-$  and  $\partial K^+$  intercept ordinate axis at  $k^- = \frac{\eta - \eta_s}{\pi \gamma_w}$  and  $k^+ = \frac{\eta - \eta_c}{\pi \gamma_w}$ , respectively.

The phenomenon of wave-breaking should also be taken into account by restricting to triples  $(H, L, h)$  belonging to the set  $H$  defined in (8). Referring to Fig. 6, the intersection  $K^- \cap H$  represents the set of triples  $(H, L, h)$  complying with the sufficient condition for seabed stability and that are physically allowable with respect to wave-breaking. Denoting by  $\bar{K}^+$  the complement of  $K^+$ , the set  $\bar{K}^+ \cap H$  stands therefore for the triples  $(H, L, h)$  that are allowable with respect to wave-breaking but causing seabed instability.

The strength capacities of the purely cohesive soil, defined by Tresca yield condition (15), is governed by the cohesion gradient. According to definition (60) of and recalling that is independent of the later parameter, domains and respectively increase and decrease as increases. In the general case, represents the critical value of for which the convex boundary and the concave boundary of are tangent, whereas reduces to the empty set (see Fig. 7). Consequently, condition may be viewed as a seabed stability criterion against the most severe wave loading.

In the static conditions  $k_v = k_h = k_1 = k_2 = 0$ , the sets  $K^-$  and  $K^+$  defined in (60) are coincident. Hence,

$$K = \left\{ (H, L, h), \frac{H}{L} \leq \frac{\eta - \gamma' \sin \theta}{\pi \gamma_w} \cosh 2\pi \frac{h}{L} \right\} \quad (61)$$

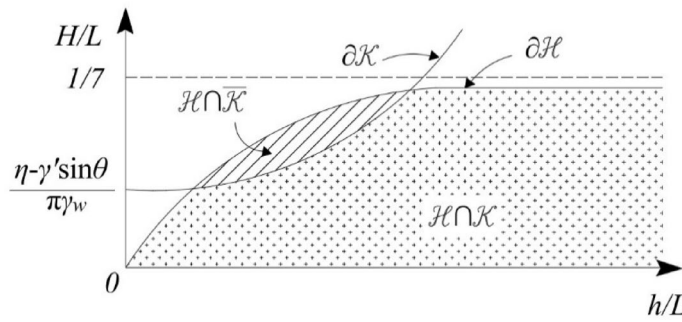


Fig. 8. Domain of allowable linear waves in the static conditions.

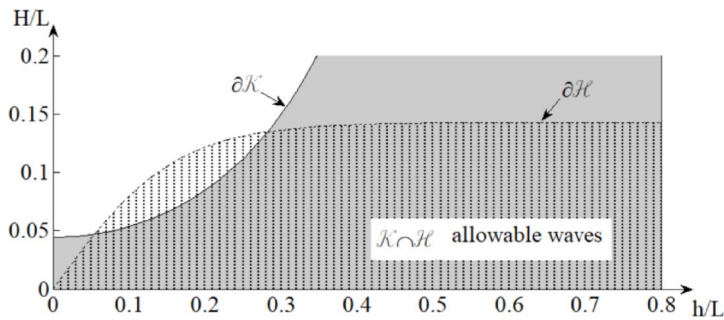


Fig. 9. Domain of allowable linear waves for horizontal seabed under static loading conditions.

Referring to Fig. 8, intersection  $K \cap H$  represents the set of triples  $(H, L, h)$  that are physically allowable with respect to wave-breaking and for which seabed stability is ensured. On the other hand, set  $\overline{K} \cap H$  is the set of wave parameters  $(H, L, h)$  that are allowable with respect to wave-breaking but causing seabed instability.

Finally, it can be observed that the critical value of  $\eta$  reads in the static case as  $\eta^* \simeq 0.225\gamma_w$ .

**Illustrative numerical application**

For illustrative purposes, the configuration of horizontal seabed (i.e.,  $\theta = 0$ ) with purely cohesive soil is addressed in this section. Emphasis is particularly devoted in the application to underline the destabilizing effect of seismic loading. The considered model data is summarized as follows<sup>45</sup>: soil cohesion gradient  $\eta = 1.4kPa/m$ , soil specific weight  $\gamma = 15.5kPa$ , water specific weight  $\gamma_w = 10kPa$ .

Neglecting the effect of vertical seismic coefficient on the seabed stability conditions (i.e.,  $k_v = 0$ ), it can be therefore shown that domain  $K$  of wave parameters  $(H, L, h)$  for which stability is ensured while complying with the wave-breaking criterion is defined by

$$K \cap H = \left\{ (H, L, h), \frac{H}{L} \leq \min \left( \frac{\eta - \gamma k_h}{\pi \gamma_w} \cosh 2\pi \frac{h}{L}, \frac{1}{7} \tanh 2\pi \frac{h}{L} \right) \right\} \tag{62}$$

It appears that the seabed stability is closely related to the numerical value of  $\eta - \gamma k_h$ . More precisely,

- If  $k_h \leq \frac{\eta}{\gamma} \approx 0.09$ , which implies  $\eta - \gamma k_h \geq 0$ , the above domain is not empty and there will exist wave loading that do not cause seabed instability. This is notably the case of stability problem under static loading conditions  $k_h = 0$  as depicted in Fig. 9.
- In contrast, when  $k_h > \frac{\eta}{\gamma} \approx 0.09$  implying  $\eta - \gamma k_h < 0$ , domain  $K \cap H$  reduces to the empty set:

$$K \cap H = \emptyset \tag{63}$$

meaning that any allowable wave will lead to seabed instability.

**Stability analysis of a granular seabed – effective stress analysis**

In granular seabed soil masses, the effect of pore pressure is expected to reveal fundamental in the stability analysis. In particular, pore pressure generated in the porous medium by wave cyclic loading and associated seepage forces may significantly reduce the seabed stability. The latter cannot therefore be relevantly addressed in the context of total stress analysis, and pore pressure shall be explicitly referred to in the limit analysis problem.

In complement to the stress boundary condition (2), the subsequent analysis assumes that the fluid pressure  $p(x, z, t)$  prevailing in the porous medium is continuous through the sea-seabed interface  $z = 0$ . The

distribution of excess pore pressure  $u$  in the porous medium, defined as the difference in pore pressure with respect to the hydrostatic value:

$$u(x, z, t) = p(x, z, t) - \gamma_w [h(x) - z \cos \theta] \quad (64)$$

should therefore comply with the following boundary condition:

$$u(x, z = 0, t) = p_{wave}(x, t) = p_0 \sin \psi \quad (65)$$

with  $\psi = \lambda x - \omega t$ .

### Formulation of the limit analysis stability problem

The purpose of this section is to describe the formulation of limit analysis problem within the context of effective stress concept validity. Such a framework of analysis explicitly emphasizes the role of water pore pressure as well as seepage forces developing during wave propagation on the seabed stability conditions. The formulation relies upon the fundamental assumption that the strength properties of the saturated soil mass are controlled by Terzaghi effective stress tensor  $\underline{\underline{\sigma}}' = \underline{\underline{\sigma}} + p \underline{\underline{1}}$ :

$$f(\underline{\underline{\sigma}}, p) = f(\underline{\underline{\sigma}}' = \underline{\underline{\sigma}} + p \underline{\underline{1}}) \leq 0 \quad (66)$$

A theoretical discussion on the validity of effective stress concept for the strength of saturated porous media is provided in de Buhan and Dormieux<sup>48</sup>. Under this assumption, the stability condition (11) of the seabed under applied loading mode is reformulated in terms of effective stresses as

$$\text{Stability} \Leftrightarrow \exists \underline{\underline{\sigma}}' \text{ such that } \begin{cases} \text{div} \underline{\underline{\sigma}}' + \gamma_e \underline{\underline{e}}_v - \text{grad } p + \gamma_e \underline{\underline{e}}_a = 0 & \text{in } \Omega \\ \underline{\underline{T}}' = \underline{\underline{T}}^d + p \underline{\underline{e}}_z & \text{along } z = 0 \\ f(\underline{\underline{\sigma}}') \leq 0 & \text{in } \Omega \end{cases} \quad (67)$$

In the above stability condition, the surface forces  $\underline{\underline{T}}^d$  acting along the boundary  $z = 0$  are given by (2), whereas the pore pressure distribution expresses  $p(x, z = 0, t) = p_{wave}(x, t) + \gamma_w h(x)$ . It follows that the stress-boundary condition can be written in terms of effective stress vector as

$$\underline{\underline{T}}' = \underline{\underline{\sigma}} \cdot \underline{\underline{n}} = 0 \text{ along } z = 0 \quad (68)$$

On the other hand, the pore pressure gradient appearing in the local equilibrium equation can be calculated from the gradient of excess pore pressure distribution:

$$\text{grad } p = \text{grad } u + \gamma_w \underline{\underline{e}}_v \quad (69)$$

The stability condition (67) is therefore reformulated in the following equivalent form:

$$\text{Stability} \Leftrightarrow \exists \underline{\underline{\sigma}}' \text{ such that } \begin{cases} \text{div} \underline{\underline{\sigma}}' + \gamma' \underline{\underline{e}}_v + \gamma_e \underline{\underline{e}}_a + \gamma_w \underline{\underline{i}} = 0 & \text{in } \Omega \\ \underline{\underline{T}}' = 0 & \text{along } z = 0 \\ f(\underline{\underline{\sigma}}') \leq 0 & \text{in } \Omega \end{cases} \quad (70)$$

where  $\gamma' = \gamma - \gamma_w$  is the buoyant unit weight and vector  $\underline{\underline{i}}$  refers to the hydraulic gradient field:

$$\underline{\underline{i}} = -\frac{1}{\gamma_w} \text{grad } u \quad (71)$$

The above formulation of the stability condition in the context of effective stresses indicates that the seepage forces can be regarded as external body forces equal to  $\gamma_w \underline{\underline{i}}$ . These driving forces of the hydraulic flow network are derived from the gradient of excess pore pressure distribution  $-\text{grad } u$  and are related to filtration velocity through Darcy's law:

$$\underline{\underline{v}} = \underline{\underline{k}} \cdot \underline{\underline{i}} = -\underline{\underline{k}} \cdot \text{grad } \frac{u}{\gamma_w} \quad (72)$$

where  $\underline{\underline{k}}$  is the soil permeability tensor (having the dimension of a velocity). In the framework of effective stress formulation, the loading mode can thus be symbolically represented by vector  $\underline{\underline{Q}} = (\gamma' \underline{\underline{e}}_v, \gamma_e \underline{\underline{e}}_a, \gamma_w \underline{\underline{i}})$ , the effective surface forces acting upon the seabed upper boundary being null  $\underline{\underline{T}}'^d = 0$ . It is recalled that the loading component  $\gamma_e \underline{\underline{e}}_a$  associated with pseudo-static forces is defined by (12).

Once the strength capacities of the soil mass are prescribed by means of the yield condition  $f(\underline{\underline{\sigma}}') \leq 0$ , the limit analysis problem (70) emphasizes that evaluation of the seepage forces  $\gamma_w \underline{\underline{i}} = -\text{grad } u$  is crucial for assessing the seabed stability condition. From a rigorous poromechanics viewpoint, the evaluation of fluid flow through the porous medium and associated seepage forces requires solving a fully coupled problem involving mutual interaction between pore pressure and skeleton strains<sup>49,50</sup>. However, the seepage forces associated with water fluid flow are evaluated in most rock and soil stability analyses from the solution to uncoupled hydraulic problem. The seepage forces that are computed independently of the skeleton deformation are then incorporated

as prescribed external body forces in the effective stability analysis (e.g.<sup>30,31,51,52</sup>). Unfortunately, such a decoupled procedure cannot be used in the present seabed stability analysis to evaluate the seepage forces induced by the wave cyclic loading. As emphasized in Dormieux et al.<sup>18</sup> and Pecker et al.<sup>53</sup>, the pore pressure generated in the granular porous medium by the wave cycles as well as associated seepage forces are fully coupled to the skeleton irreversible strains. The progressive pore pressure build-up is closely related to irreversible volume changes of the porous material reflecting the granular soil densification. In that respect, the formulation of a simplified framework specifically devised for evaluating the seepage forces involved in the seabed stability problem will be addressed in next Sect. 4.2.

As regards the strength properties of the granular seabed soil modeled as a homogeneous and isotropic material, a cohesionless Mohr-Coulomb yield criterion will be adopted throughout the subsequent effective stress analysis:

$$f(\underline{\sigma}') = \sup \{ \sigma'_i (1 + \sin \phi) - \sigma'_j (1 - \sin \phi) \mid i, j = 1, 2, 3 \} \leq 0 \tag{73}$$

where  $\sigma'_i$  with  $i \in \{1, 2, 3\}$  are the effective principal stresses. The strength parameter  $\phi$  is the internal friction angle.

### Theoretical uncoupled framework for assessing pore pressure generation (Dormieux et al., 1993)

In the effective stress formulation, the seepage forces  $\gamma_w \underline{i} = -\text{grad } u$  act as external force that should be previously evaluated. For this purpose, we resort in the present analysis to the theoretical framework originally formulated by Dormieux<sup>17</sup> and Dormieux et al.<sup>18</sup>. The basic idea of this modeling consists in splitting the time scale into two well separated scales respectively associated with the wave cyclic loading of period  $T = \frac{2\pi}{\omega}$  (fast time scale) and the characteristic time of fluid time diffusion in the porous medium  $T_c$  (slow time scale).

The fundamental assumptions of the modeling can be summarized as follows:

- The solid and fluid particles of the porous medium are incompressible. The seabed porous medium is considered as a homogeneous and isotropic material undergoing infinitesimal transformations.
- The reference state of the seabed soil mass is defined by an “initial” stress state  $\underline{\sigma}_0$  equilibrating the gravity forces  $\gamma \underline{e}_v$  and associated pseudo-static component  $\gamma \underline{e}_a$ , together with the hydrostatic pressure forces  $\underline{T}_0^d = \gamma_w h(x) \underline{e}_z$  acting along the upper seabed boundary  $z = 0$ . The “initial” pore pressure is hydrostatic, that is  $p_0 = \gamma_w [h(x) - z \cos \theta]$ .
- Pore pressure generation is equal to the excess pore pressure  $u$  induced by wave cyclic loading. In particular, pore pressure build-up resulting from earthquake sequences is disregarded in the analysis (e. g., Pecker et al.<sup>53</sup>).
- Under the assumption of infinitesimal skeleton transformation, the behavior of the seabed constituent relates the variation of effective stress  $\delta \underline{\sigma} + u \underline{1}$  with respect to initial state to the skeleton strain  $\underline{\underline{\varepsilon}} = 1/2 (\nabla \underline{\xi} + {}^t \nabla \underline{\xi})$  associated with displacement  $\underline{\xi}$ :

$$\delta \underline{\sigma} + u \underline{1} = \mathbb{C} : \left( \underline{\underline{\varepsilon}} - \frac{1}{3} \varepsilon_v^{ir} \underline{1} \right) \tag{74}$$

where  $\varepsilon_v^{ir}$  denotes irreversible volumetric strain and the fourth-order tensor  $\mathbb{C}$  refers to the drained elastic stiffness moduli. The introduction of inelastic volumetric strains reflects the difference from a purely poroelastic behavior and represents a fundamental feature of the pore pressure build-up model. In addition, the volumetric behavior is assumed to be exclusively contractive:

$$\dot{\varepsilon}_v^{ir} \leq 0 \tag{75}$$

Such a contractancy condition is associated in saturated granular materials with the increase of pore pressures.

In order to evaluate the excess pore pressure distribution  $u$  as well as the variations in stress field  $\delta \underline{\sigma}$  resulting from the wave overpressure  $p_{wave}(x, t)$ , the starting point of the model proposed in Dormieux et al.<sup>18</sup> is the time scale separation commonly satisfied for typical waves and marine sediments:

$$T/T_c \ll 1 \tag{76}$$

where the characteristic time of fluid mass diffusion is evaluated as  $T_c = L^2/c_m$ . The fluid diffusivity coefficient  $c_m$  is related to soil permeability and oedometric elastic modulus by

$$c_m = E_{oed} \frac{k}{\gamma_w} \quad \text{with} \quad E_{oed} = K + \frac{4}{3}G \tag{77}$$

where  $K$  and  $G$  are respectively the drained elastic bulk and shear moduli. Parameter  $k$  stands for the soil permeability coefficient.

During the periodic wave loading, the excess pore pressure  $u$  is expected to be a quasi-periodic function of time, oscillating with the wave period  $T$  around a mean value, which varies only at the scale of the characteristic time of consolidation  $T_c$  (Fig. 10). Relying upon the scale separation (74) and a two-time scale expansion technique, Dormieux et al.<sup>18</sup> established that the excess pore pressure  $u$  can be split into two uncoupled contributions:

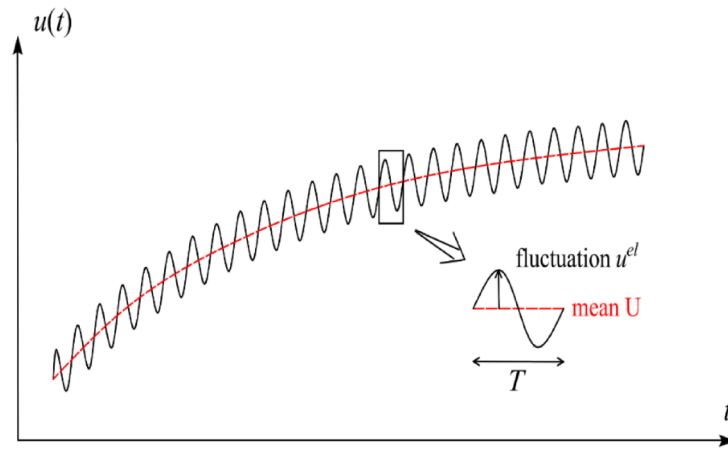


**Fig. 10.** Schematic representation of excess pore pressure variations viewed as quasi-periodic function of time.

$$u = u^{el} + U \tag{78}$$

where  $u^{el}$  is the periodic poroelastic fluctuation with average equal to zero over the wave period  $T$  and  $U$  is the drift term corresponding to the mean value of  $u$  over one cycle of period  $T$ . The component  $u^{el}$  is a function of the fast time variable, whereas the component  $U$  representing the progressive pore pressure build-up depends only on the slow time variable. It is convenient to introduce the elastic and irreversible parts of the hydraulic gradient  $\underline{i} = \underline{i}^{el} + \underline{i}^{ir}$ :

$$\underline{i}^{el} = -\frac{1}{\gamma_w} \text{grad } u^{el} \quad \text{and} \quad \underline{i}^{ir} = -\frac{1}{\gamma_w} \text{grad } U \tag{79}$$

The homologous decomposition of strain and stress variations reads

$$\begin{cases} \delta \underline{\underline{\sigma}} = \delta \underline{\underline{\sigma}}^{el} + \delta \underline{\underline{\Sigma}} \\ \delta \underline{\underline{\varepsilon}} = \delta \underline{\underline{\varepsilon}}^{el} + \underline{\underline{\varepsilon}} \end{cases} \tag{80}$$

Evaluation of  $u^{el}$  and  $U$  as well as associated hydraulic gradient fields  $\underline{i}^{el}$  and  $\underline{i}^{ir}$ , together with that of stress variation fields  $\delta \underline{\underline{\sigma}}^{el}$  and  $\delta \underline{\underline{\Sigma}}$ , will be discussed in the next section.

**Formulation of the wave-induced poroelastic response**

The periodic pore pressure fluctuation  $u^{el}$  and stress variation  $\delta \underline{\underline{\sigma}}^{el}$  are solutions to a poroelastic problem stated on the seabed subjected to wave cyclic loading  $p_{wave}(x, t)$ . The state Eq. (74) relating the effective stress variation  $\delta \underline{\underline{\sigma}}^{el} + u^{el} \underline{\underline{1}}$  to the skeleton strain  $\delta \underline{\underline{\varepsilon}}^{el}$  reduces to the poroelastic relationship:

$$\delta \underline{\underline{\sigma}}^{el} + u^{el} \underline{\underline{1}} = \mathbb{C} : \underline{\underline{\varepsilon}}^{el} \tag{81}$$

The poroelastic boundary value problem is defined by the following governing equation:

- (i) The constitutive state Eq. (81).
- (ii) The quasi-static momentum balance equation for the porous continuum:

$$\text{div } \delta \underline{\underline{\sigma}}^{el} = 0 \tag{82}$$

- (iii) The diffusion equation relating skeleton volumetric strains and pore pressure:

$$\frac{\partial}{\partial t} \text{tr } \underline{\underline{\varepsilon}}^{el} = \frac{k}{\gamma_w} \nabla^2 u^{el} \tag{83}$$

where  $\nabla^2$  denotes the Laplacian operator.

- (iv) The boundary conditions along the seabed surface and impervious substrate:

$$\begin{cases} \delta \underline{\underline{\sigma}}^{el} \cdot \underline{e}_z = -p_{wave} \underline{e}_z, & u^{el} = p_{wave} & \text{at } z = 0 \\ \underline{\xi} = 0, & \frac{\partial u^{el}}{\partial z} = 0 & \text{at } z = -d \end{cases} \quad (84)$$

For a seabed layer with infinite thickness, the boundary conditions at  $z = -d$  should be replaced by conditions  $\underline{\xi} = 0$  and  $u^{el} = 0$  at  $|z| \rightarrow \infty$ .

Based on the two-scale expansion technique, Dormieux et al.<sup>15</sup> and Pecker et al.<sup>42</sup> have shown that the skeleton volumetric strain is subjected to no fluctuation during a time scale of wave period  $T \ll T_c$ , that is  $\frac{\partial}{\partial t} \text{tr} \underline{\underline{\xi}}^{el} = 0$ . Consideration of the latter property in the diffusion Eq. (83) implies that the periodically fluctuating pore pressure is harmonic.

The construction of closed-form solution to the above poroelastic problem has been addressed by Quiuqui et al.<sup>35</sup> in the case of horizontal seabed (i.e.,  $\theta = 0$ ). These authors extended the work developed in Hsu and Jeng<sup>54</sup> to account for inertial effects and fluid compressibility. Resorting to the complex variable method, the obtained expressions for pore pressure and stress fields are summarized below:

$$u^{el} = -\frac{1}{1-2\nu} \text{Re} \left\{ \left[ (1-2\nu) (C_1 e^{\lambda z} - C_2 e^{-\lambda z}) + (1-\nu) (\lambda'^2 - \lambda^2) (C_3 e^{\lambda' z} + C_4 e^{-\lambda' z}) \right] i \bar{p} \right\} \quad (85)$$

and

$$\delta \underline{\underline{\sigma}}^{el} = -u^{el} \underline{\underline{1}} + z \frac{\partial u^{el}}{\partial z} (\underline{e}_z \otimes \underline{e}_z - \underline{e}_x \otimes \underline{e}_x) + z \frac{\partial u^{el}}{\partial x} (\underline{e}_x \otimes \underline{e}_z + \underline{e}_z \otimes \underline{e}_x) \quad (86)$$

where ‘Re’ stands for the real part,  $\nu$  is the soil Poisson ratio and  $\bar{p} = p_0 e^{i(\lambda x - \omega t)}$  is the complex representation of wave overpressure  $p_{wave}$ . Complex parameter  $\lambda'$  is related to the wave number and soil properties through the following relationship

$$\lambda'^2 = \lambda^2 - i \frac{\omega \gamma_w}{k} \frac{1-2\nu}{2G(1-\nu)} \quad (87)$$

Expressions of the four complex coefficients  $(C_i)_{1 \leq i \leq 4}$  depending on soil properties, wave parameters and seabed geometry are provided in Appendix A.

As regards the hydraulic gradient  $\underline{\underline{i}}^{el} = -\text{grad } u^{el} / \gamma_w$  associated with the poroelastic fluctuation, which represents the periodic component of seepage forces in the seabed stability analysis, its expression is given by

$$\underline{\underline{i}}^{el} = -\frac{p_0}{\gamma_w (1-2\nu)} \left[ \lambda (-H_u(z) \cos \psi + J_u(z) \sin \psi) \underline{e}_x - (H_u'(z) \sin \psi + J_u'(z) \cos \psi) \underline{e}_z \right] \quad (88)$$

where expressions of the non-dimensional functions  $H_u(z)$  and  $J_u(z)$  are also provided in Appendix A. Functions  $H_u'(z)$  and  $J_u'(z)$  refer to the derivatives of  $H_u(z)$  and  $J_u(z)$ , that is  $H_u' = \partial H_u / \partial z$  and  $J_u' = \partial J_u / \partial z$ .

In the case of seabed with infinite thickness, the above pore pressure solution simplifies to

$$u_{\infty}^{el} = p_0 e^{\lambda z} \sin(\lambda x - \omega t) \quad (89)$$

while the stress variation  $\delta \underline{\underline{\sigma}}_{\infty}^{el}$  is still computed from  $u_{\infty}^{el}$  by relationship (84). The elastic hydraulic gradient simply reads:

$$\underline{\underline{i}}^{el} = -\frac{\lambda p_0}{\gamma_w} e^{\lambda z} (\cos \psi \underline{e}_x + \sin \psi \underline{e}_z) \quad (90)$$

Full details on the construction of such poroelastic solution may be found in Quiuqui et al.<sup>35</sup>.

For illustrative purposes, the above poroelastic pore pressure fluctuation and associated hydraulic gradient are depicted in Figs. 11 and 12 considering several values for the normalized thickness  $d/L$  of seabed layer. The set of parameters used for numerical illustrations is listed in Table 1. The values of the wave crest to trough height  $H$  and the wave length  $L$  are computed by means of expressions (5)–(7).

Figure 11 displays the profiles of excess pore pressure fluctuation  $u^{el}$  in the soil mass for the different soil layer thicknesses:  $d/L \in \{0.25, 0.5, 1, \infty\}$ . The configuration  $d/L \rightarrow \infty$  corresponds to the seabed with infinite thickness analyzed in Dormieux and Coussy<sup>28</sup>. For the sake of clarity, the distribution of  $u^{el}$  obtained in the latter configuration is plotted using bullet symbols. The distributions shown in this figure refer to the maximum excess pore pressure value obtained under the wave crest (i.e.,  $\psi = \pi/2$ ). It is first observed that the predictions of pore pressure fluctuation are quite similar to the finite element solutions obtained by Gatmiri<sup>55</sup>. As it could be expected, the vertical profile of  $u^{el}$  is significantly affected by the value of seabed normalized thickness as long as  $d/L \leq 1$ . For higher values of seabed thickness, say typically  $d/L > 1$ , the excess pore pressure distribution closely approximates the infinite depth solution. In those cases, the solution (89) can be accurately used to approximate the profile of  $u^{el}$  in the soil mass (i.e.,  $u^{el} \approx u_{\infty}^{el}$ ). Regardless of considered ratio  $d/L$ , the distribution of excess pore pressure in the seabed layer monotonically decreases with depth from the upper surface  $z = 0$  with a change in the vertical profile curvature near the impervious base  $z = -d$ .

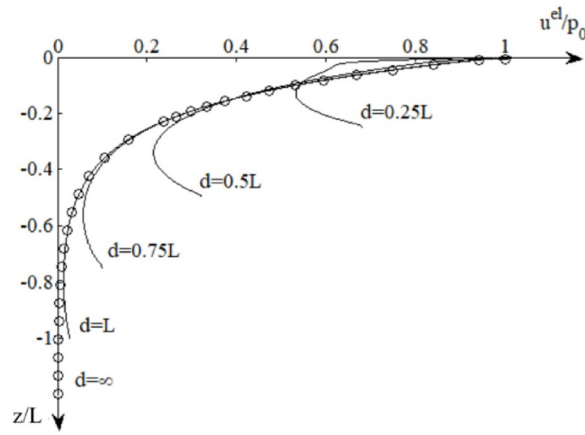


Fig. 11. Profiles of normalized wave-induced pore pressure in the soil mass.

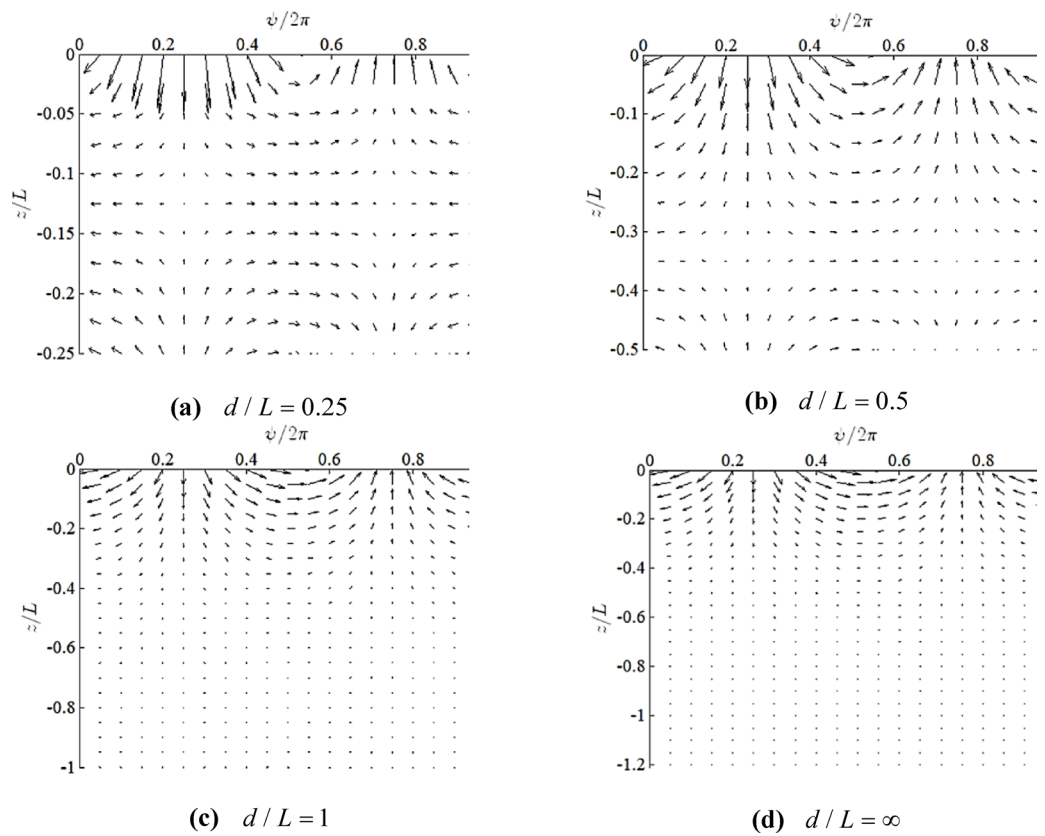


Fig. 12. Normalized seepage forces  $\gamma_w \xi^{el}/p_0$  in the soil mass for different values of normalized soil layer thickness.

Soil properties	Wave characteristics	Geometry
$k = 10^{-4}$ m/s	$T = 10$ s	$h = 15$ m
$G = 10$ MPa	$H_0/L_0 = 0.06$	$d/L = 0.25, 0.5, 1, \infty$
$\nu = 1/3, \gamma' = \gamma_w = 10$ kN/m <sup>3</sup>	$p_0 = 31.3$ kPa	

Table 1. Model parameters for the numerical illustrations of wave-induced poroelastic response.

Figure 12 presents the plots of normalized seepage forces  $-\text{grad } u^{el}/p_0 = \gamma_w \dot{\underline{\varepsilon}}^{el}/p_0$  obtained for the different soil layer thicknesses. In all of  $d/L$  cases, the magnitude of the seepage force vector is maximum at the upper surface  $z = 0$  and decreases with depth, the direction of this vector being vertical downward under the wave crest and vertical upward under the wave troughs. It is also observed that the change in curvature of the pore pressure profile near the impervious base  $z = -d$  is reflected by a change in the seepage force direction.

Granular soil densification and associated pore pressure build-up take place under cyclic shear loadings. In that respect, let denote by  $\delta \underline{\underline{\sigma}}^{el} = \delta \underline{\underline{\sigma}}^{el} - 1/3 \text{tr } \underline{\underline{\sigma}}^{el}$  the periodically fluctuation of deviatoric stress and by

$$J_2^{el} = \sqrt{\frac{1}{2} \delta \underline{\underline{\sigma}}^{el} : \delta \underline{\underline{\sigma}}^{el}}$$

the corresponding second invariant that characterizes the amplitude of shear stresses.

Based on the two-time scale expansion reasoning, Dormieux et al.<sup>18</sup> showed that the magnitude of cyclic shear loading governing soil contractancy in the seabed can be measured by

$$\pi^{el} = \max_{\psi} \sqrt{J_2^{el}} \tag{91}$$

Figure 13 displays the profiles of normalized cyclic shear loading  $\tau^{el}/p_0$  induced in the seabed soil mass by wave overpressure considering the set parameters provided in Table 1. For finite layer thickness (i.e.,  $d/L < \infty$ ) the maximum shear loading  $\tau^{el}$  is obtained under a wave node of wave (i.e.,  $\psi = \pi/2$ ). For infinite thickness seabed  $d/L = \infty$ ,  $J_2^{el}$  is independent of the  $\psi$  variable.

The analysis of the results shown in Fig. 7 indicates that for small  $d/L$  ratios, such as  $d/L = 0.25$ , the shear stress  $\tau^{el}$  reaches its maximum at the seabed interface with impervious base  $z^* = d$  with  $\tau^{el}(z^*) \approx 0.45 p_0$ . In contrast, for higher values of ratio  $d/L$ , typically  $d/L \geq 0.75$ , the maximum value is achieved close to seabed upper surface at a depth around  $z^* \approx 0.16 L$  with  $\tau^{el}(z^*) \approx 0.36 p_0$ . It is also observed that the shear stress  $\tau^{el}$  vanishes at the seabed-base interface as soon as  $d/L \geq 1$  and the prediction reveals very close to that obtained for infinite layer thickness.

Although the poroelastic solution ( $u^{el}, \delta \underline{\underline{\sigma}}^{el}$ ) has been derived in the case of horizontal seabed (i.e.,  $\theta = 0$ ), it will however be used in the stability analysis as a first approximation for inclined seabed with small angle  $\theta \ll 1$ .

### Evaluation of inelastic hydraulic gradient

Evaluation of the seepage forces  $\gamma_w \dot{\underline{\varepsilon}}^{ir} = -\text{grad } U$  associated with the drift component  $U$  of excess pore pressure introduced in (78) stems theoretically from the solution to a poromechanical boundary value problem stated on the seabed material system in terms of the mean quantities  $U$  and  $\delta \underline{\underline{\Sigma}}$  over one cycle loading. By definition, the fields involved in such a poromechanical problem depend only on the slow time variable  $\bar{t} = t/T_c$ .

In consistency with the state Eq. (74) formulated for the behavior of the soil material constituent, the relationship between the mean stress  $\delta \underline{\underline{\Sigma}}$  and strain  $\underline{\underline{\varepsilon}}$  tensors reads

$$\underline{\underline{\Sigma}} + U \underline{\underline{1}} = \mathbb{C} : \left( \underline{\underline{\varepsilon}} - \frac{1}{3} \varepsilon_v^{ir} \underline{\underline{1}} \right) \tag{92}$$

As previously stated, the introduction of contractive irreversible volumetric strain  $\varepsilon_v^{ir} = \varepsilon_v^{ir}(\bar{t})$  reflecting material densification at the slow time scale (controlled by  $T_c$ ) is an essential feature in the model formulated by Dormieux et al.<sup>18</sup> for predicting pore pressure build-up under wave cyclic loading.

The slow scale diffusion equation of the pore pressure  $U$  takes the following form:

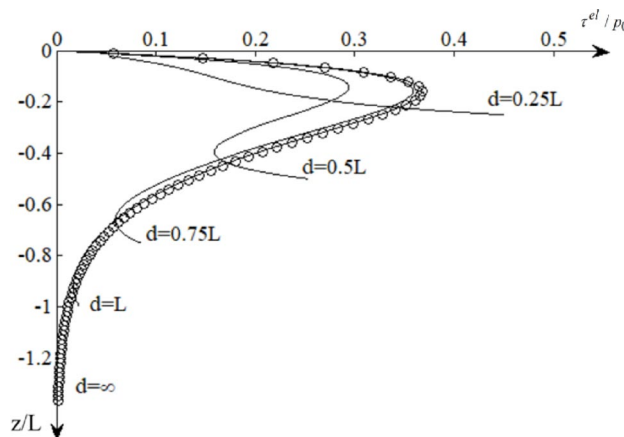


**Fig. 13.** Profiles of the normalized shear stress  $\tau^{el}/p_0$  in the soil mass for different values of normalized soil layer thickness.

$$\frac{\partial U}{\partial \bar{t}} = c_m T_c \nabla^2 U - K \frac{\partial \varepsilon_v^{ir}}{\partial \bar{t}} \quad (93)$$

in which the source term  $-K \frac{\partial \varepsilon_v^{ir}}{\partial \bar{t}}$  represents the rate of generated pore pressure associated with the irreversible volumetric strain rate  $\frac{\partial \varepsilon_v^{ir}}{\partial \bar{t}}$ . A simple reasoning based on the analysis of the variations of  $\varepsilon_v^{ir}$  with respect to the slow time variable indicates that the increment  $\Delta \varepsilon_v^{ir}$  over a loading cycle (i.e. drift value during a wave period) can be approximated as

$$\Delta \varepsilon_v^{ir} \approx \frac{T}{T_c} \frac{\partial \varepsilon_v^{ir}}{\partial \bar{t}} \quad (94)$$

Accordingly, the diffusion equation governing the time and space variations of the excess pore pressure  $U$  may then be rearranged in the form

$$\frac{1}{T_c} \frac{\partial U}{\partial \bar{t}} = c_m \nabla^2 U - K \Delta \varepsilon_v^{ir} / T \quad (95)$$

In addition, the pore pressure  $U$  is subjected to the following boundary conditions:

$$\begin{cases} U = 0 & \text{at } z = 0 \\ \frac{\partial U}{\partial z} = 0 & \text{at } z = -d \end{cases} \quad \forall \bar{t} \quad (96)$$

together with zero initial condition

$$U = 0 \quad \text{for } \bar{t} = 0 \quad (97)$$

The remaining equations defining the boundary value problem consist of the field momentum balance law:

$$\text{div } \underline{\underline{\Sigma}} = 0 \quad (98)$$

and mechanical boundary conditions:

$$\begin{cases} \underline{\underline{\Sigma}} \cdot \underline{e}_z = 0 & \text{at } z = 0 \\ \underline{\underline{\xi}} = 0 & \text{at } z = -d \end{cases} \quad (99)$$

Being the displacement associated with the strain tensor field  $\underline{\underline{\varepsilon}}$ .

In the above poromechanical boundary value problem, the irreversible volumetric strain  $\varepsilon_v^{ir}$  appears as the characteristic of the loading in the boundary value problem formulated in terms of mean-quantities. In that respect, let us consider for a while that field  $\varepsilon_v^{ir}$  is known. In that case, the problem under consideration can be viewed as a poroelastic problem with a prescribed strain source term. Provided that field  $\varepsilon_v^{ir}$  is independent of the spatial coordinate  $x$ , the structure of the mean-quantities problem indicates that the solution  $(U, \underline{\underline{\Sigma}})$  will be itself independent of  $x$ . Once the distribution of excess pore pressure  $U$  is computed from Eqs. (95), (96) and (97), the stress solution  $\underline{\underline{\Sigma}}$  is then given by

$$\underline{\underline{\Sigma}} = \underline{\underline{\Sigma}} (\underline{e}_x \otimes \underline{e}_x + \underline{e}_y \otimes \underline{e}_y) \quad \text{with } \underline{\underline{\Sigma}} = -\frac{1-2\nu}{1-\nu} (K \varepsilon_v^{ir} + U) \quad (100)$$

In anticipation of further developments that will be provided in this section, it is useful to calculate the expression of mean effective stress:

$$\frac{1}{3} \text{tr} (\underline{\underline{\Sigma}} + U \underline{\underline{1}}) = -\frac{2}{3} \frac{1-2\nu}{1-\nu} K \varepsilon_v^{ir} + \frac{1}{3} \frac{1+\nu}{1-\nu} U \quad (101)$$

The solution  $(U, \underline{\underline{\Sigma}})$  of the above poroelastic problem as well as the irreversible hydraulic gradient  $\underline{\underline{i}}^{ir} = -\frac{1}{\gamma_w} \text{grad } U$  are therefore determined as a functional of  $\varepsilon_v^{ir}$ , which should be evaluated beforehand based on the numerous experimental works that have been developed to provide a quantitative description of soil contractancy under cyclic loading. A review of relevant literature on this topic may be found for instance in Pecker<sup>56</sup>, Dormieux<sup>17</sup> or in the recent contribution by Wichtmann et al.<sup>57</sup>, to cite a few. The idea consists basically of evaluating the increment  $\Delta \varepsilon_v^{ir}$  of irreversible volumetric strain caused by the  $N^{\text{th}}$  loading cycle as a function of the cyclic shear amplitude  $\tau^{cl}$  given by (91), of the mean effective stress  $\sigma'_m$  during the cycle number  $N$  and the contractancy  $\varepsilon_v^{ir, N-1}$  accumulated along the previous  $N-1$  cycles. In this context, the following experimental-based model proposed by Dormieux<sup>17</sup> and extended later in Dormieux et al.<sup>18</sup> is adopted in this analysis:

$$\Delta \varepsilon_v^{ir} = F (S' \varepsilon_{v, N-1}^{ir}) = - \frac{\bar{\kappa}}{\bar{\alpha}} S^{\bar{\beta}} \exp \left( \frac{\bar{\beta} - 1}{\bar{\kappa}} \varepsilon_{v, N-1}^{ir} \right) \tag{102}$$

where  $\bar{\alpha}$ ,  $\bar{\beta}$  and  $\bar{\kappa}$  are material parameters. The stress ratio  $S'$  is defined from the shear stress amplitude and effective mean stress by

$$S' = \frac{\tau^{el}}{|\sigma'_m|} \quad \text{with} \quad \sigma'_m = \frac{1}{3} \text{tr} \underline{\sigma}' + \frac{1}{3} \text{tr} (\underline{\Sigma} + U \underline{1}) \tag{103}$$

The first term in the expression of  $\sigma'_m$  refers to the initial effective mean stress, whereas the second term is given by Eq. (101) and represents the contribution of the effective stress solution to the inelastic problem. Neglecting the contribution of the pseudo-static component  $\gamma e_a$  of the gravity forces and considering the lagged value of  $\sigma'_m$  yields

$$S' \approx \frac{\tau^{el}}{|\sigma'_{m, N-1}|} \quad \text{with} \quad \sigma'_{m, N-1} = \frac{1 + 2\bar{K}_0}{3} \gamma' z_v - \frac{2}{3} \frac{1 - 2\nu}{1 - \nu} K \varepsilon_{v, N-1}^{ir} + \frac{1}{3} \frac{1 + \nu}{1 - \nu} U_{N-1} \tag{104}$$

in which the value of term  $\frac{1}{3} \text{tr} (\underline{\Sigma} + U \underline{1})$  in Eq. (101) is computed at cycle and  $z_v = x \sin \theta + z \cos \theta$  is the vertical depth. Parameter  $\bar{K}_0$  refers to the coefficient of earth pressure at rest, classically introduced to define the geostatic initial stress state  $S'$ .

Owing to the assumption of slight inclination of the seabed  $\theta \ll 1$ , the approximation  $z_v \approx z$  allows to consider as a first approximation that  $\varepsilon_v^{ir}$  as well as the solution  $(U, \underline{\Sigma})$  to inelastic problem are independent of coordinate  $x$ , i.e.  $\varepsilon_v^{ir} = \varepsilon_v^{ir}(z, \bar{t})$ ,  $U = U(z, \bar{t})$  and  $\underline{\Sigma} = \underline{\Sigma}(z, \bar{t})$ , so that the hydraulic gradient is parallel takes the expression  $\underline{i}^{ir} = i^{ir}(z, \bar{t}) \underline{e}_z$  with  $i^{ir} = -\frac{1}{\gamma_w} \frac{\partial U}{\partial z}$ .

The preceding analysis that has been developed to address the problem governing the mean stress and effective pore pressure distributions is based on the assumption of homogeneous soil properties, which might reveal restrictive since stiffness and permeability generally vary with depth. The predictions derived from the modeling should therefore be interpreted in the context of such limiting assumption.

### Numerical results – excess pore pressure generation

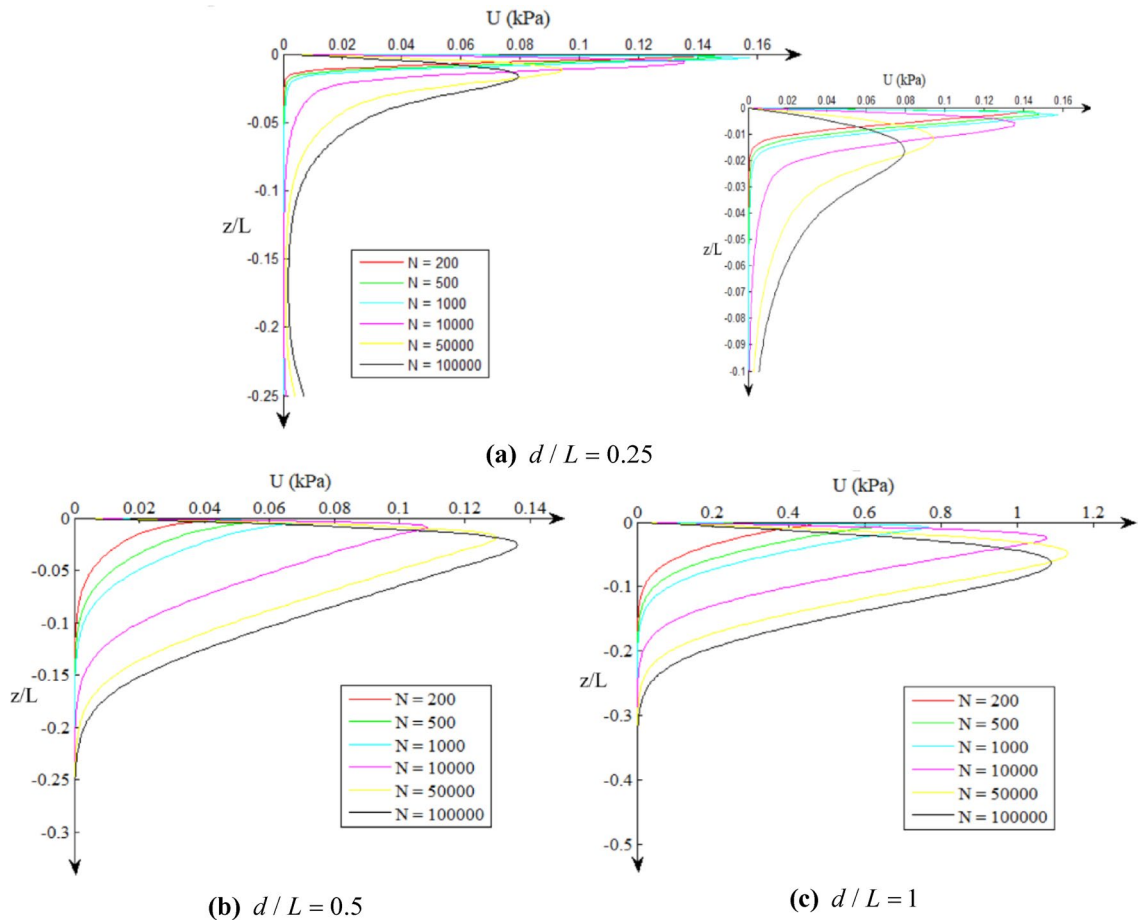
This section provides some numerical results that illustrates the model predictions for excess pore pressure generation  $U$  in the seabed soil mass as well as associated hydraulic gradient that defines the seepage forces in the effective stress stability problem. The set of governing Eqs. (95)–(97) together with experimental-based expression (102) of irreversible volumetric strain increment  $\Delta \varepsilon_v^{ir}$  are numerically solved resorting to an explicit finite difference procedure implemented in MATLAB software. The numerical simulations consider the model parameters given in Table 2<sup>18</sup>. The initial state of stresses is assumed to be isotropic, i.e.  $K_0 = 1$ . It is important to emphasize that the primary objective herein is not to provide quantitative numerical results, but only to illustrate the trends of  $U$  and  $\underline{i}^{ir}$  profiles within the seabed soil mass. The spatial discretization along the seabed depth (vertical direction) consists of regularly distributed nodes with constant spacing  $\Delta h = \min(d/100, 0.25 \text{ m})$ . A time step increment  $\Delta t = \min(T_c^{num}/2, T/1000)$  is adopted in the time stepping algorithm, the numerical characteristic time of fluid mass diffusion being computed as  $T_c^{num} = \Delta h^2/c_m$ . For each selected model data, the numerical simulations are carried out over progressively increasing time spans until the hydraulic gradient  $i^{ir}(0)$  reaches a quasi-stationary value.

Figure 14 displays the distribution of irreversible excess pore pressure along the seabed depth. For each thickness ratio  $d/L$ , the distributions of  $U$  are shown for wave cycles ranging from  $N = 200$  to  $N = 100000$ . It is pointed out that the number of cycles represents a measure of the slow time variable  $\bar{t}$ . Prior to results analysis, two preliminary observations should first be stated:

- Regarding the effects of bed thickness, the model predictions of pore pressure generated in a seabed with infinite thickness reveal very close to those computed in the case  $d/L = 1$ .
- In comparison with the results provided in Dormieux<sup>17</sup> and Dormieux et al.<sup>18</sup>, the pore pressure profiles obtained from the numerical simulations exhibit similar shapes with, however, lower values in terms of predicted pressure accumulation. This discrepancy is mainly attributed to the fact the present model operates with homogeneous soil modulus, whereas the above-mentioned studies considered a soil bulk modulus that increases with depth.

Soil properties	Wave characteristics	Geometry
$c_m = 10^{-3} \text{ m}^2 \text{ s}^{-1}$	$T = 10 \text{ s}$	$h = 15 \text{ m}$
$K = 27 \text{ MPa} \nu = 1/3$	$H_0/L_0 = 0.06$	$d/L = 0.25, 0.5, 1, \infty$
$\bar{\alpha} = 0.0023 \bar{\beta} = 6.644 \bar{\kappa} = 0.005 \gamma' = \gamma_w = 10 \text{ kN/m}^3$	$p_0 = 31.3 \text{ kPa}$	

**Table 2.** Model parameters for the numerical illustrations of inelastic response.



**Fig. 14.** Distributions of Profiles of normalized wave-induced pore pressure in the soil mass.

The results of Fig. 14 indicate a gradual pore pressure build-up as the loading cycles proceed. For a given loading cycle, the excess pore pressure increases with depth  $|z|$  within a crust lying near the upper seabed boundary. More precisely, it increases from  $U = 0$  at the surface  $z = 0$  and reaches its maximum value at a point defined by coordinate  $z = z^*$  located near the seabed boundary. For higher depths  $z \leq z^*$ , the distribution of pore pressure exhibits a decreasing profile with depth. In terms of seepage forces, it follows from the above observation that  $\gamma_w i^{ir} e_z = -\frac{\partial U}{\partial z} e_z$  is oriented upward (toward the upper seabed surface) within region  $z^* \leq z \leq 0$  and downward (toward the seabed base) in the region  $-d \leq z \leq z^*$ . Accordingly, the seepage forces would act as destabilizing (resp, stabilizing) loading component in the upper region  $z^* \leq z \leq 0$  (resp, in region  $-d \leq z \leq z^*$ ). Referring to the stability analysis that will be carried out in Sect. 4.6, a risk of surface instability may be associated with excess pore pressure accumulation in the region close to upper surface. In that respect, it seems therefore relevant to evaluate the variations of irreversible hydraulic gradient  $i^{ir}(z = 0)$  along the loading cycles. Figure 15 displays the results computed for each value of the ratio  $d/L$ . After an increasing phase with the cycle number  $N$ , the magnitude of hydraulic gradient  $i^{ir}(0)$  reaches a plateau followed by a phase of gradual decrease. The latter phase is likely a consequence of experimental-based model (102) expressing a decrease of  $\Delta \varepsilon_v^{ir}$  with densification.

To conclude with and in anticipation of the effective stress stability problem handled in Sect. 4.6, the following property deduced from the general form of pore pressure profiles:

$$\forall z \in [0, z^*] \quad i^{ir}(z, \bar{t}) = -\frac{1}{\gamma_w} \frac{\partial U}{\partial z} \geq 0 \quad \text{and} \quad \int_z^0 i^{ir}(z, \bar{t}) dz = \frac{1}{\gamma_w} U(z = 0, \bar{t}) \geq 0 \quad (105)$$

will be used to compute the rate of work performed by seepage forces in the context of kinematic approach implementation. The above property stems from the condition  $U = 0$  at the surface  $z = 0$  and the fact the derivative  $\frac{\partial U}{\partial z}$  is a negative and decreasing function for  $z^* \leq z \leq 0$ .

**Effective stress-based upper bound kinematic approach**

The stability problem (70) formulated in the context of effective stresses may be addressed either by the lower static approach or by the upper bound kinematic approach. The conjunction of the two approaches allows for

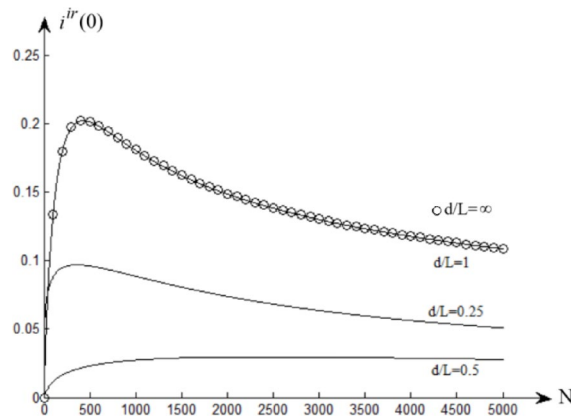


**Fig. 15.** Evolution of irreversible hydraulic gradient at the seabed surface  $z = 0$  with increasing number of loading cycles.

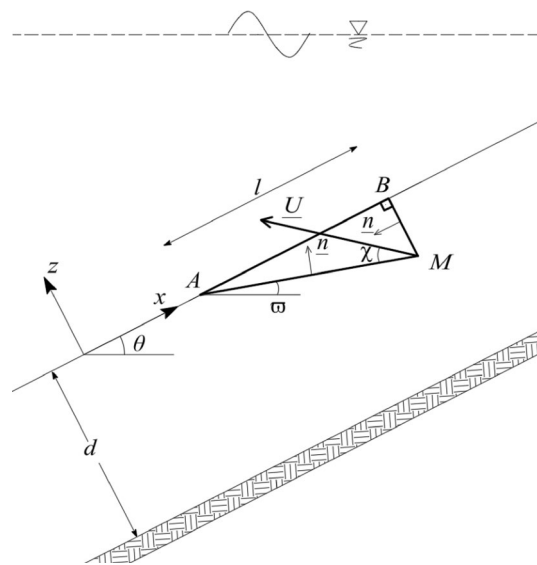


**Fig. 16.** Geometry of the translational failure mechanism.

bracketing the convex domain  $K$  of safe loads. In the case of a granular soil mass, the lower static approach would require the formulation of effective stress and excess pore pressure distributions complying in the seabed layer with the equilibrium and strength conditions, which is not an easy task. Unlike the case of purely cohesive seabed soil analyzed in Sect. 3, the stability analysis developed for the granular soil mass will actually be restricted to the formulation of an upper bound estimate for convex  $K$  based on the implementation of a class of failure mechanisms. The basic idea of the present kinematic approach is to seek for a virtual failure mechanism that reproduces the surface instability induced by seepage forces in the region close to bed upper surface.

The class of failure mechanism considered in the study consists of a triangular wedge  $MAB$  in uniform translation motion  $\underline{U}$ , whereas the remaining part of the seabed ground is kept motionless. Referring to Fig. 16, such a failure mechanism is defined by the geometrical parameters  $\varpi$ ,  $l = AB$  and the inclination  $\chi$  of  $\underline{U}$  with respect to sides  $MA$ . Regarding the geometry definition of wedge  $MAB$ , the previous angular parameters are subjected to the following constraints:

$$-\frac{\pi}{2} + \theta < \varpi < \theta \tag{106}$$

The vertex  $M$  of the triangular block in translation is chosen close to the upper surface so that its coordinate  $z_M$  lies in the region  $z^* \leq z_M \leq 0$ . Such a failure mechanism involves velocity discontinuities  $[\underline{U}] = \underline{U}$  inclined at angle  $\chi$  with respect to lines  $MA$  and  $MB$ . The translation velocity of the triangular wedge is given by

$$\underline{U} = U [-\cos(\chi + \theta - \varpi) \underline{e}_x + \sin(\chi + \theta - \varpi) \underline{e}_z] \tag{107}$$

The necessary stability condition of the seabed under applied loading is derived by applying the fundamental kinematic inequality (37) to the above failure mechanism. For this purpose, it is necessary to compute the expressions of maximum resisting work rate  $P_{mr}(\underline{U})$  and external work rate  $P_{ext}(\underline{U})$  developed in the failure mechanism. The rate of maximum resisting work comprises two contributions associated with the velocity jump along lines  $MA$  and  $MB$ :

$$P_{mr}(\underline{U}) = \int_{MA} \Pi(\underline{n}, [\underline{U}]) ds + \int_{MB} \Pi(\underline{n}, [\underline{U}]) ds \tag{108}$$

where  $[\underline{U}] = \underline{U}$  and  $\underline{n}$  refers in both above integrals to a unit normal vector to the lines  $MA$  and  $MB$ , respectively. The support function associated with the cohesionless Mohr-coulomb strength criterion  $f(\underline{\sigma}') \leq 0$  defined in (73) are computed as<sup>20,21</sup>:

$$\Pi(\underline{n}, \underline{U}) = \sup \left\{ \underline{U} \cdot \underline{\sigma}' \cdot \underline{n} \mid f(\underline{\sigma}') \leq 0 \right\} = \begin{cases} \Pi(\underline{n}, \underline{U}) = +\infty & \text{if } \underline{U} \cdot \underline{n} < U \sin \phi \\ \Pi(\underline{n}, \underline{U}) = 0 & \text{if } \underline{U} \cdot \underline{n} \geq U \sin \phi \end{cases} \tag{109}$$

It is therefore necessary to satisfy condition  $\underline{U} \cdot \underline{n} \geq U \sin \phi$  along both the discontinuity lines  $MA$  and  $MB$  for the considered kinematic approach to provide non-trivial upper bound solutions. It is readily that such a condition is achieved by imposing the following restriction:

$$\begin{cases} \phi \leq \chi \leq \pi - \phi \\ |\chi + \theta - \varpi| \leq \frac{\pi}{2} - \phi \end{cases} \tag{110}$$

which should be fulfilled in conjunction with the geometry restrictions (106) to achieve an effective kinematic approach. In that case, the rate of maximum resisting work reduces to  $P_{mr}(\underline{U}) = 0$  and the kinematic theorem (37) yields the following necessary condition for stability:

$$P_{ext}(\underline{U}) \leq P_{mr}(\underline{U}) = 0 \tag{111}$$

that should be satisfied for any set of parameters  $(\varpi, l, \chi)$  complying with conditions (106) and (110). It is noted that conditions (110) reduce to the following restriction regarding the velocity jump inclination:

$$\phi \leq \chi \leq \frac{\pi}{2} - \phi + \varpi - \theta \tag{112}$$

In the framework of effective stress stability formulation (67), the rate of external work  $P_{ext}(\underline{U})$  includes the contributions of gravity forces  $\gamma' \underline{e}_v$  (gravity minus buoyancy), seismic components associated with the gravity forces  $\gamma \underline{e}_a$  and seepage forces  $\gamma_w \underline{i} = \gamma_w \underline{i}^{el} + \gamma_w \underline{i}^{ir}$ :

$$P_{ext}(\underline{U}) = \int_{MAB} \gamma' \underline{e}_v \cdot \underline{U} dS + \int_{MAB} \gamma \underline{e}_a \cdot \underline{U} dS + \int_{MAB} \gamma_w \underline{i}^{el} \cdot \underline{U} dS + \int_{MAB} \gamma_w \underline{i}^{ir} \cdot \underline{U} dS \tag{113}$$

The two first integral terms of the right-hand side are easily computed as

$$\begin{cases} \int_{MAB} \gamma' \underline{e}_v \cdot \underline{U} dS = -U S \gamma' \sin(\chi - \varpi) \\ \int_{MAB} \gamma \underline{e}_a \cdot \underline{U} dS = U S \gamma [k_h \cos(\chi - \varpi) - k_v \sin(\chi - \varpi)] \end{cases} \tag{114}$$

where  $S = \frac{l^2}{2} \tan(\theta - \varpi)$  stands for the area of triangle  $MAB$ . Recalling that the irreversible part of the hydraulic gradient takes the form  $\underline{i}^{ir} = i^{ir}(z, \bar{t}) \underline{e}_z$ , the corresponding contribution to the rate of external work reads

$$\int_{MAB} \gamma_w \underline{i}^{ir} \cdot \underline{U} dS = U \gamma_w \sin(\chi + \theta - \varpi) \int_{MAB} i^{ir} dS \tag{115}$$

As regards the contribution of the elastic part  $\underline{i}^{el}$ , it follows from (88) that

$$\int_{MAB} \gamma_w \underline{i}^{el} \cdot \underline{U} dS = -U \frac{p_0}{1 - 2\nu} \left\{ \cos(\chi + \theta - \varpi) \int_{MAB} A_u dS + \sin(\chi + \theta - \varpi) \int_{MAB} B_u dS \right\} \tag{116}$$

where functions  $A_u$  and  $B_u$  are defined as  $A_u = H_u(z) \cos \psi - J_u(z) \sin \psi$  and  $B_u = -H_u'(z) \sin \psi - J_u'(z) \cos \psi$ . Similarly to  $\underline{i}^{el}$ , these functions are functions of the two space coordinates  $(x, z)$  and of the time  $t$  (or fast time variable  $t/T$ ).

Before further developments, it should be recalled that spatial distributions of  $\underline{i}^{el}$  and  $\underline{i}^{ir}$  depend on the value of seabed thickness.

Substituting the above expressions into (113), inequality (111) reads

$$-\gamma' \sin(\chi - \varpi) + \gamma [k_h \cos(\chi - \varpi) - k_v \sin(\chi - \varpi)] + \gamma_w \sin(\chi + \theta - \varpi) \langle i^{ir} \rangle - \frac{p_0}{1 - 2\nu} \{ \cos(\chi + \theta - \varpi) \langle A_u \rangle + \sin(\chi + \theta - \varpi) \langle B_u \rangle \} \leq 0 \quad (117)$$

in which symbol  $\langle \cdot \rangle$  denotes the average value over the area  $MAB$ :

$$\langle \cdot \rangle = \frac{1}{S} \int_{MAB} \cdot dS \quad (118)$$

The most critical stability condition derived from considered class of failure mechanisms is obtained by maximizing the left-hand side in the above inequality with respect to the set of parameters  $(\varpi, l, \chi)$  complying with conditions (106) and (112) and to  $\psi \in [0, 2\pi]$ .

It is first observed from Eq. (105) that  $\langle i^{ir} \rangle$  is a positive number and that number  $\sin(\chi + \theta - \varpi)$  takes only positive values within the considered range of angular parameters. Taking into account the properties of function  $i^{ir}(z, \bar{t})$  expressed at the end of the preceding section, it can be readily shown, by invoking for instance the mean value theorem, that close the upper seabed surface  $\langle i^{ir} \rangle$  is, for a fixed value of  $\varpi$ , a decreasing function of length  $l$ . More precisely,

$$\max_l \langle i^{ir} \rangle = \lim_{l \rightarrow 0} \langle i^{ir} \rangle = i^{ir}(0) \quad (119)$$

Regarding the two terms of inequality (117) that are related to the contribution of elastic hydraulic gradient, a reasoning analogous to that followed by Dormieux et al.<sup>18</sup> is adopted in the present analysis, admitting the following property:

$$\forall l \geq 0 \quad U = -\frac{p_0}{1 - 2\nu} \{ \cos(\chi + \theta - \varpi) \langle A_u \rangle + \sin(\chi + \theta - \varpi) \langle B_u \rangle \} \leq \lim_{l \rightarrow 0} U \quad (120)$$

After some algebraic developments, the analytical expression of  $\lim_{l \rightarrow 0} U$  is derived as:

$$\lim_{l \rightarrow 0} U = -p_0 \{ \cos(\chi + \theta - \varpi) \lambda [\Upsilon_1 \cos \psi - \Upsilon_2 \sin \psi] - \sin(\chi + \theta - \varpi) [\Upsilon_3 \sin \psi + \Upsilon_4 \cos \psi] \} \quad (121)$$

where parameters  $(\Upsilon_i)_{1 \leq i \leq 4}$  are defined in Appendix B. The value  $\psi^*$  of  $\psi$  that achieves the maximum of above expression is equal to

$$\psi^* = \arctan \frac{\lambda \Upsilon_2 + \Upsilon_3 \tan(\chi + \theta - \varpi)}{-\lambda \Upsilon_1 + \Upsilon_4 \tan(\chi + \theta - \varpi)} \quad (122)$$

Substituting (122) into (121) and taking into account (119), the necessary stability condition (117) can be reformulated as follows

$$\gamma_w \sin(\chi + \theta - \varpi) i^{ir}(0) \leq \gamma' \sin(\chi - \varpi) + \gamma [-k_h \cos(\chi - \varpi) + k_v \sin(\chi - \varpi)] - p_0 \cos(\chi + \theta - \varpi) \sqrt{\{-\lambda \Upsilon_1 + \Upsilon_4 \tan(\chi + \theta - \varpi)\}^2 + \{\lambda \Upsilon_2 + \Upsilon_3 \tan(\chi + \theta - \varpi)\}^2} \quad (123)$$

which should be satisfied for any values of the angular parameters  $\varpi$  and  $\chi$  complying with conditions (106) and (112). In particular, adopting  $\varpi \rightarrow \theta$  and  $\chi = \phi$  yields:

$$\gamma_w i^{ir}(0) \leq \frac{1}{\sin \phi} (\gamma' \sin(\phi - \theta) - \Lambda \lambda p_0 - \gamma k^*) \quad (124)$$

where coefficients  $\Lambda$  and  $k^*$  are defined as

$$\Lambda = \sqrt{\left(-\Upsilon_1 \cos \phi + \frac{\Upsilon_4}{\lambda} \sin \phi\right)^2 + \left(\Upsilon_2 \cos \phi + \frac{\Upsilon_3}{\lambda} \sin \phi\right)^2} \quad (125)$$

$$k^* = k_h \cos(\phi - \theta) - k_v \sin(\phi - \theta) \quad (126)$$

Inequality (124) represents the necessary stability condition for the seabed under applied loading that can be derived from investigate class of failure mechanisms. It extends the results obtained by Dormieux et al.<sup>18</sup> for a seabed with infinite thickness (i.e.  $d \rightarrow \infty$ ) under static conditions (i.e.  $k_v = k_h = 0$ ). In that case, it can be shown that  $\lim_{d \rightarrow \infty} (\Upsilon_1, \Upsilon_2, \Upsilon_3, \Upsilon_4) = (1, 0, \lambda, 0)$  and the stability condition (124) reduces to

$$\gamma_w i^{ir}(0) \leq \frac{\gamma' \sin(\phi - \theta) - \lambda p_0}{\sin \phi} \quad (127)$$

### Geometrical interpretation of the stability condition

The necessary stability condition (124) derived in the context of the limit analysis kinematic approach allows to formulate an upper bound approximation  $K^c$  of the stability domain  $K$  defined in Eq. (14). For a fixed set of seismic coefficients ( $k_h, k_v$ ) and soil to water unit weight ratio  $\gamma/\gamma'$ , it is convenient for the graphical representation to characterize the loading mode by means of two dimensionless components  $\underline{Q} = (Q_1 = \frac{\lambda p_0}{\gamma}, Q_2 = \frac{\gamma_w}{\gamma'} i^{ir}(0))$ , so that inequality (124) is rewritten as

$$\frac{\Lambda}{\sin(\phi - \theta)} Q_1 + \frac{\sin \phi}{\sin(\phi - \theta)} Q_2 \leq 1 - \frac{\gamma/\gamma'}{\sin(\phi - \theta)} k^* \tag{128}$$

and associated upper bound domain  $K^c$  is

$$K \subseteq K^c = \left\{ \underline{Q}; \frac{\Lambda}{\sin(\phi - \theta)} Q_1 + \frac{\sin \phi}{\sin(\phi - \theta)} Q_2 \leq 1 - \frac{\gamma/\gamma'}{\sin(\phi - \theta)} k^* \leq 0 \right\} \tag{129}$$

It is pointed out that the components of the loading  $\underline{Q}$  can be interpreted as follows. Parameter  $Q_1 = \frac{\lambda p_0}{\gamma}$  directly reflects the wave loading intensity, whereas  $Q_2 = \frac{\gamma_w}{\gamma'} i^{ir}(0)$  represents the action of seepage forces associated with the irreversible volumetric strains caused by the cyclic loading. The geometrical domain describing the set  $K^c$  in the plane ( $Q_1, Q_2$ ) is sketched in Fig. 17. The bounds  $Q_1^+$  and  $Q_2^+$  appearing in the latter figure are defined as

$$Q_1^+ = \frac{\sin(\phi - \theta) - \gamma/\gamma' k^*}{\Lambda}, \quad Q_2^+ = \frac{\sin(\phi - \theta) - \gamma/\gamma' k^*}{\sin \phi} \tag{130}$$

Referring to the plane ( $Q_1, Q_2$ ),  $K^c$  represents the set of loads that are potentially withstand by the seabed, in the sense any loading lying outside this domain will certainly cause seabed instability.

In order to briefly illustrate the destabilizing effect induced by seismic loading, we consider the configuration of a horizontal seabed (i.e.,  $\theta = 0$ ) with layer thickness  $d \in \{0.25 L, 0.5 L, L, \infty\}$  and soil friction angle fixed to  $\phi = 30^\circ$ . The additional parameters required for computing coefficient  $\Lambda$  defined in (124) are given in Table 2. Neglecting the effect of vertical seismic coefficient on the seabed stability conditions (i.e.,  $k_v = 0$ ), Fig. 18 emphasizes the reduction of domain  $K^c$  for increasing values of horizontal seismic coefficient  $k_h$ . In particular, a loading that is potentially sustained by the bed under static conditions  $k_h = 0$ , such as the loading represented by vector  $\underline{Q}^*$  in Fig. 18, will certainly cause seabed instability as soon as  $k_h \geq 0.1$  whatever the value of considered ratio  $d/L$ . The results of Fig. 18 also corroborates the fact that the  $K^c$  prediction strongly depends on the seabed thickness for  $d/L \leq 1$ , whereas it coincides with the prediction obtained for infinite depth layer as soon as  $d/L \geq 1$ .

Following a reasoning similar to that developed in Sect. 3 for purely cohesive soil mass, it is convenient for practical applications to characterize the set  $K$  of wave parameters ( $H, L, h$ ) for which the seabed stability is ensured. It follows from expressions (4) defining the wave overpressure amplitude together with the kinematic approach (124) that

$$K \subseteq K^+ = \left\{ (H, L, h), \frac{H}{L} \leq k^+ \cosh 2\pi \frac{h}{L} \right\} \tag{131}$$

with

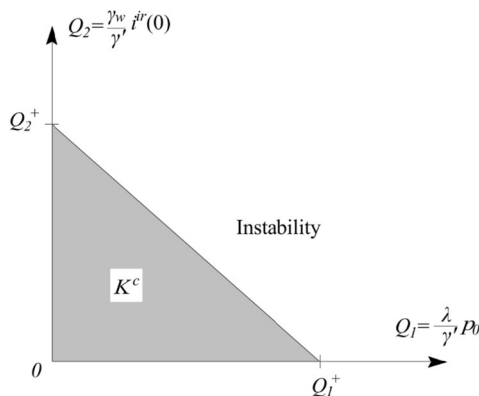


**Fig. 17.** Schematic representation of the upper bound kinematic approximation  $K^c$  of stability domain in the plane ( $Q_1, Q_2$ ).

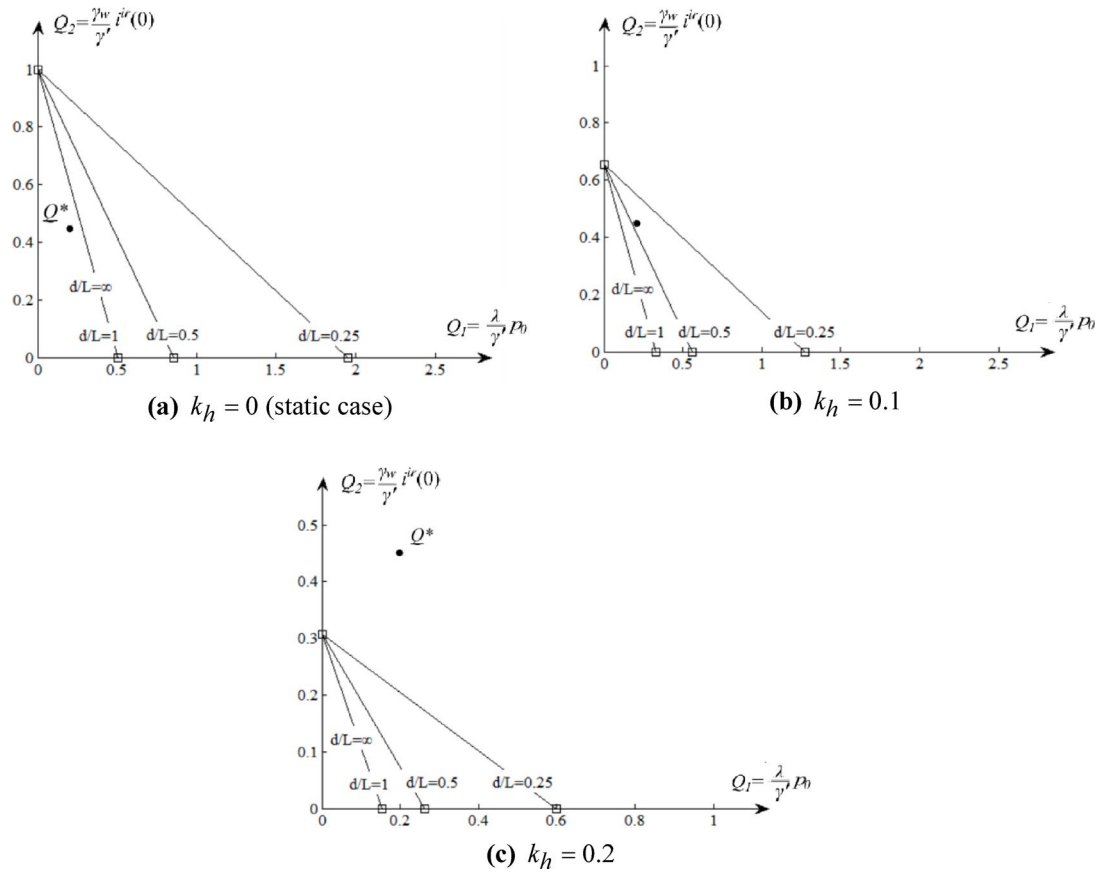


Fig. 18. Effect of the horizontal seismic coefficient on the upper bound estimate  $K^c$  in plane  $(Q_1, Q_2)$ .

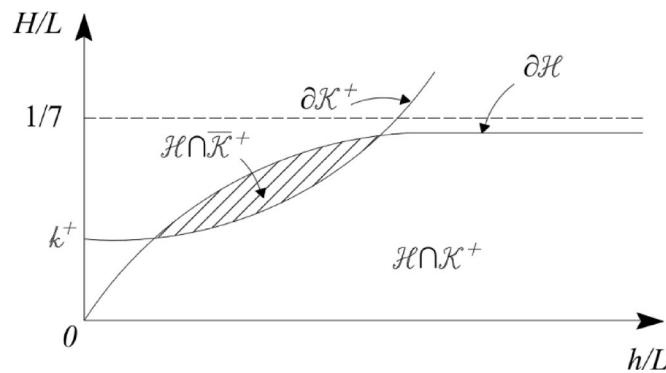


Fig. 19. Domain defining allowable linear waves in the plane  $(H/L, h/L)$  for granular soil.

$$k^+ = \frac{\gamma' \sin(\phi - \theta) - \gamma_w i^{in}(0) \sin \phi - \gamma k^*}{\Lambda \pi \gamma_w} \tag{132}$$

The above definition of set  $K^+$  implicitly assumes that all quantities necessary for computing the dimensionless parameter  $k^+$  are prescribed. Additionally, the phenomenon of wave-breaking should also be considered by restricting to triples  $(H, L, h)$  belonging to the set  $H$  defined in (8). Referring to the plane  $(h/L, H/L)$ , the upper bound estimate  $K^+$  of  $K$  as well as the set  $H$  are plotted in Fig. 19.

The intersection  $H \cap K$  represents the set of triples  $(H, L, h)$  complying with the necessary stability condition and that are physically allowable with respect to wave-breaking. As far as the seabed stability is concerned, the triples of  $(H, L, h)$  cannot be rigorously referred to as safe waves. Introducing the complement set  $\bar{K}^+$  of  $K^+$ , the set  $\bar{K}^+ \cap H$  represents therefore the triples  $(H, L, h)$  that are allowable with respect to wave-breaking but causing seabed instability.

## Conclusion

The limit analysis reasoning has been implemented to investigate the stability of a seabed subjected to the combined action of water waves and seismic loading. The effects of water wave on submerged bed are addressed in the context of first-order Stokes theory by means of a periodic overpressure propagating along the sea floor surface. Following the standard approach adopted in engineering stability analyses, the concept of pseudo-static inertia forces is used to account for the inertial forces developed in the soil mass, presumably generated by the earthquake ground motion. The limit analysis problem governing seabed stability is handled within the context of total stress analysis, appropriate for clayey or low permeability silty soils, as well as in the framework of effective stress, which is relevant for granular materials.

In the case of a purely cohesive seabed whose strength capacities are described by a Tresca failure condition with depth-varying cohesion, total stress stability analysis is carried out by implementing static and kinematic approaches. The seabed stability conditions have been expressed in terms of loading parameters and alternatively in terms of allowable wave parameters.

For granular seabed soil masses, the stability analysis relies upon the formulation of limit analysis in the context of effective stresses, which requires to be able to properly evaluating the seepage forces associated with the gradient of excess pore pressure distribution generated in the soil mass by the cyclic wave action. Extending the simplified framework originally set up in Dormieux et al.<sup>18</sup>, the hydraulic gradient, which represents a fundamental loading component for the stability analysis, can be evaluated as the sum of a poroelastic fluctuation over the wave period and a drift term associated with irreversible soil densification under the shear cyclic wave loading. The numerical illustration showed that both the poroelastic and irreversible parts of seepage forces can significantly depend on the layer thickness  $d$  as long as the latter remains smaller than the wavelength  $L$ .

Once the simplified framework for evaluating the seepage forces is set up, the limit analysis kinematic approach has then been implemented by means of a class of virtual failure. The upper bound prediction based on the approach is clearly interpreted as a necessary condition for the seabed stability under applied loading. It appears from the formulation that the relevant loading parameter reflecting the effects of seepage forces is the value of irreversible hydraulic gradient along the seabed surface. The kinematic predictions implicitly depend on the seabed thickness since the distributions of poroelastic and irreversible hydraulic gradients are affected by this parameter.

A natural extension of the analysis to be foreseen in the future refers to the formulation of a static approach to obtain lower bound solutions for the stability of granular seabed soil mass. Such formulation is currently the object of ongoing research. Further developments should also account for the contribution of pseudo-static surface loading  $\underline{T}_a^d$  in the stability analysis. In the context of pseudo-static method, this can be by computing the corresponding rate of work  $\int_{\Omega} \underline{T}_a^d \cdot \underline{U} d\Omega$ , which should be included in the expression of the rate of work  $P_{ext}(\underline{U})$  performed by the external loads.

The deterministic pseudo-static analysis developed in the paper should be viewed as a preliminary approach to the seismic seabed stability. Among the limitations of such a simplified framework of analysis one may quote:

- Unlike dynamic response analyses that consider the whole acceleration time history (e.g.<sup>58,59</sup>), the pseudo-static approach cannot account for cyclic shear strength degradation, as well as the pore pressure generation/dissipation induced by earthquake sequences.
- The deterministic seabed stability assessment disregards the inherent spatial variability of soil mass strength and permeability properties. It is recommended that such an approach be complemented by probabilistic and reliability-based stability analyses. In that respect, stochastic and probabilistic formulations that account for uncertainties in soil parameters appear suitable for more realistic and improved seabed stability analyses. In that respect, representative works on the topic include references<sup>58,60–65</sup>.
- The kinematic approach implemented in the seabed stability analysis relies, in both purely cohesive and granular soil mass, upon failure mechanisms defined by translational triangular wedges. Despite their simplicity, such failure mechanisms have proven accurate for assessing seabed stability under static conditions, as they provide upper bound solutions that are close to the lower bound estimates<sup>47</sup>. However, seabed failure modes associated with earthquake loading, prescribed via acceleration time history, would likely involve more complex failure mechanisms than the translational triangular failure mechanisms. The idea to address this issue would consist in seeking the form of failure surface through minimization procedure of the stability condition, analogous to that developed in Ceron et al.<sup>69</sup> for the stochastic stability analysis of slopes subjected to seepage forces.

## Data availability

The data that support the findings of this study are available from the corresponding author upon reasonable request.

Received: 16 May 2025; Accepted: 3 December 2025

Published online: 09 December 2025

## References

1. Jouffray, J. B., Blasiak, R., Norström, A. V., Österblom, H. & Nyström, M. The blue acceleration: the trajectory of human expansion into the ocean. *One Earth*. 2 (1), 43–54 (2020).

2. He, R., Kaynia, A. M., Zheng, J. & Zhang, J. Effect of gap and scour on dynamic behavior of monopiles and offshore wind structures. *Ocean Eng.* **243**, 110336 (2022a).
3. He, R., Zhang, J. & Zheng, J. Vertical dynamic interaction factors for offshore thin-walled pipe piles. *Comput. Geotech.* **145**, 104656 (2022b).
4. Hance, J. J. Submarine slope stability. In *Development of a Database and Assessment of Seafloor Slope Stability based on Published Literature*. Project report prepared for the Minerals Management Service under the MMS/OTRC Cooperative Research Agreement 1435-01-99-CA-31003, Task Order 18217, MMS Project 421 (2003).
5. Cui, L. & Jeng, D. S. Numerical study for stability of a cross-anisotropic seabed around a harbor entrance under random waves. In ISOPE International Ocean and Polar Engineering Conference (ISOPE-I). ISOPE (2022).
6. Wang, G., Liu, Y., Liu, K. & Xu, C. Dynamic response and liquefaction potential of porous seabed induced by partial standing ocean waves. *Sci. Rep.* **13** (1), 19061 (2023).
7. Lin, J., Gao, Y., Guo, Y., Liu, J. & Feng, L. Wave-induced sloping seabed residual response around a buried pipeline. *Mar. Georesources Geotechnol.* **43** (7), 1355–1373 (2025).
8. Sassa, S. & Sekiguchi, H. Analysis of wave-induced liquefaction of sand beds. *Geotechnique* **51** (2), 115–126 (2001).
9. Chen, W. Y., Chen, G. X., Chen, W., Liao, C. C. & Gao, H. M. Numerical simulation of the nonlinear wave-induced dynamic response of anisotropic poro-elastoplastic seabed. *Mar. Georesources Geotechnol.* **37** (8), 924–935 (2019).
10. Ye, J., Jeng, D., Wang, R. & Zhu, C. Numerical simulation of the wave-induced dynamic response of poro-elastoplastic seabed foundations and a composite breakwater. *Appl. Math. Model.* **39** (1), 322–347 (2015).
11. Zhao, K. et al. Wave-induced dynamics of marine pipelines in liquefiable seabed. *Coast. Eng.* **140**, 100–113 (2018).
12. Madsen, O. S. Wave-induced pore pressures and effective stresses in a porous bed. *Géotechnique* **28** (4), 377–393 (1978).
13. Yamamoto, T., Koning, H., Sellmeijer, H. & Hijum, E. On the response of a poro-elastic bed to water waves. *J. Fluid Mech.* **87** (1), 193–206 (1978).
14. Dormieux, L. & Delage, P. Effective stress response of a plane sea-bed under wave loading. *Géotechnique* **38** (n. 3), 445–450 (1988).
15. Ishihara, K. & Yamazaki, A. Analysis of wave-induced liquefaction in seabed deposits of sand. *Soils and Foundations* **24** (3), 85–100 (1984).
16. Rahman, Jaber, C. L. A simplified drained analysis for wave-induced liquefaction in ocean floor sands. *Soils and Foundations* **26** (3), 57–68 (1986).
17. Dormieux, L. Influence de la houle sur la stabilité d'un massif sous-marin. PhD thesis (in french), École Nationale des Ponts et Chaussées, Paris (1989).
18. Dormieux, L., Auriault, J. L. & Coussy, O. Pore pressures generation in a seabed subjected to wave loading. *Eur. J. Mech.* **12** (n. 6), 773–801 (1993). *A/Solids*.
19. Salençon, J. *Calcul à La Rupture Et Analyse Limite* (Presses de l'E.N.P.C., 1983).
20. Salençon, J. An introduction to the yield design theory and its application to soil mechanics. *Eur. J. Mech. A/Solids*. **9** (n°5), 477–500 (1990).
21. Salençon, J. *Yield Design* (John Wiley & Sons, Inc., 2013).
22. Seed, H. B. Considerations in the Earthquake-resistant design of Earth and rockfill dams. *Geotechnique* **29** (3), 215–263 (1979).
23. Chen, W. F. & Liu, X. L. *Limit Analysis in Soil Mechanics* (Elsevier, 1990).
24. Saada, Z., Maghous, S. & Garnier, D. Stability analysis of rock slopes subjected to seepage forces using the modified Hoek-Brown criterion. *Int. J. Numer. Anal. Methods Geomech.* **37** (18), 3194–3212 (2013).
25. Belghali, M., Saada, Z., Garnier, D. & Maghous, S. Pseudo-static stability analysis of rock slopes reinforced by passive bolts using the generalized Hoek-Brown criterion. *J. Rock Mech. Geotech. Eng.* **9** (4), 659–670 (2017).
26. Saada, Z., Chihi, O., Maghous, S. & Garnier, D. A pseudo-static approach to the seismic bearing capacity of eccentrically loaded footing lying on rock obeying a generalized Hoek-Brown strength criterion. *Arab. J. Geosci.* **16** (2), 117 (2023).
27. Dormieux, L. Stability of a purely cohesive seabed soil under wave loading. *Géotechnique*, **38**, 1, 121–123 (1988).
28. Dormieux, L. & Coussy, O. Stability of a sedimentary half-space subjected to an arbitrary pressure distribution. *Eur. J. Mech.* **10** (n. 4), 371–394 (1991). *A/Solids*.
29. Dormieux, L. Stability analysis of a seabed subjected to wave loading. *Mech. Res. Commun.* **19** (n. 4), 325–331 (1992).
30. de Buhann, P., Cuvillier, P., Dormieux, L. & Maghous, S. Face stability of shallow circular tunnels driven under the water table: A numerical analysis. *Int. J. Numer. Anal. Meth. Geomech.* **23** (1), 79–95 (1999).
31. Saada, Z., Maghous, S. & Garnier, D. Pseudo-static analysis of tunnel face stability using the generalized Hoek-Brown strength criterion. *Int. J. Rock Mech. Min. Sci.* **55**, 45–54 (2012).
32. Mei, C. C. & Foda, M. A. Wave-induced stresses around a pipe laid on a poroelastic seabed. *Géotechnique* **31** (4), 509–517 (1989).
33. Le Méhauté B. *An Introduction To Hydrodynamics and Water Waves* (Springer Science & Business Media, 2013).
34. Dean, R. G. & Dalrymple, R. A. *Water Wave Mechanics for Engineers and Scientists* Vol. 2 (World scientific publishing company, 1991).
35. Quiuqui, J. P. C., Tamayo, J. P. & Maghous, S. Closed-form solutions for wave-induced poroelastic response in seabed under dynamic and quasi-static regimes. *J. Brazilian Soc. Mech. Sci. Eng.* **44** (1), 16 (2022).
36. Sasaki, T. O. & Horikawa, K. Observation of nearshore current and edge waves. In *Proceedings of the 16th International Conference on Coastal Engineering*. ASCE, 791–809 (1978).
37. Jibson, R. W. Methods for assessing the stability of slopes during earthquakes—A retrospective. *Eng. Geol.* **122** (1–2), 43–50 (2011).
38. Papadimitriou, A. G., Bouckovalas, G. D. & Andrianopoulos, K. I. Methodology for estimating seismic coefficients for performance-based design of earthdams and tall embankments. *Soil Dyn. Earthq. Eng.* **56**, 57–73 (2014).
39. Rodríguez-Castellanos, A., Martínez-Calzada, V., Rodríguez-Sánchez, J. E., Orozco-del-Castillo, M. & Carbajal-Romero, M. *Induced Water Pressure Profiles Due To Seismic Motions* Vol. 47, 9–16 (Applied Ocean Research, 2014).
40. An, C., Cai, C., Zheng, Y., Meng, L. S. & Liu, P. Theoretical solution and applications of ocean bottom pressure induced by seismic seafloor motion. *Geophys. Res. Lett.* **44**, 10272–10281 (2017).
41. Nosov, M. et al. Relationship between pressure variations at the ocean bottom and the acceleration of its motion during a submarine earthquake. *Earth Planet Space.* **70**, 100 (2018).
42. Matsumoto, H., Kimura, T., Nishida, S., Machida, Y. & Araki, E. Experimental evidence characterizing pressure fluctuations at the seafloor-water interface induced by an earthquake. *Sci. Rep.* **8**, 16406 (2018).
43. Wang, P. G., Yu, W. L., Zhao, M. & Du, X. L. Effects of wind-wave-current-earthquake interaction on the wave height and hydrodynamic pressure based on CFD method. *Ocean Eng.* **305**, 117909 (2024).
44. Chen, Y., Huang, X., Wu, K. & Li, Z. X. Experimental research on dynamic responses and hydrodynamic pressures of deep-water Bridge piers under seismic and wave actions. *Eng. Struct.* **313**, 118276 (2024).
45. Braun, A. L., Brüch, A. & Maghous, S. A mixed 3D-1D finite element formulation for analysis of geomaterial structures with embedded curvilinear inclusions: application to load transfer in mooring anchor systems. *Latin Am. J. Solids Struct.* **15**, e103 (2018).
46. Shukha, R. & Baker, R. Design implications of the vertical pseudo-static coefficient in slope analysis. *Comput. Geotech.* **35** (1), 86–96 (2008).
47. Madalozzo, D. M. S. Contribuição à análise das instabilidades do leito oceânico induzidas pelo carregamento cíclico da onda. PhD thesis (in Portuguese). Universidade Federal do Rio Grande do Sul, Porto Alegre (2016).

48. de Buhan, P. & Dormieux, L. On the validity of the effective stress concept for assessing the strength of saturated porous materials: a homogenization approach. *J. Mech. Phys. Solids*. **44** (10), 1649–1667 (1996).
49. Coussy, O. & Poromechanics John Wiley & Sons Ltd, West Sussex (2004).
50. Dormieux, L., Kondo, D., Ulm, F. J. & Microporomechanics John Wiley & Sons Ltd, Chichester (2006).
51. Pan, Q., Xu, J. & Dias, D. Three-Dimensional stability of a slope subjected to seepage forces. *Int. J. Geomech.* **17** (8), 04017035 (2017).
52. Wang, S. T., Yang, X. L., Huang, F. & Pan, Q. J. Three-dimensional upper-bound analysis of rock slopes subjected to seepage forces based on Hoek-Brown failure criterion. *Comput. Geotech.* **138**, 104310 (2021).
53. Pecker, A., Prevost, J. H. & Dormieux, L. Analysis of pore pressure generation and dissipation in cohesionless materials during seismic loading. *J. Earthquake Eng.* **5** (04), 441–464 (2001).
54. Hsu, J. R. C. & Jeng, D. S. Wave-induced soil response in an unsaturated anisotropic seabed of finite thickness. *Int. J. Numer. Anal. Methods Geomech.* **18** (11), 785–807 (1994).
55. Gatmiri, P. A simplified finite element analysis of wave-induced effective stresses and pore pressures in permeable sea beds. *Géotechnique* **40** (1), 15–30 (1990).
56. Pecker, A. *Dynamique Des Sols* (Presses de l'ENPC, 1984).
57. Wichtmann, T., Tafili, M., Staubach, J. & Macháček, J. Soil behaviour under cyclic loading - experiments, constitutive modelling and numerical applications, Keynote Lecture. In: 10th European Conference on Numerical Methods in Geotechnical Engineering - NUMGE2023 (2023).
58. Rodriguez-Ochoa, R., Nadim, F., Cepeda, J. M., Hicks, M. A. & Liu, Z. Hazard analysis of seismic submarine slope instability. *Georisk: Assess. Manage. Risk Eng. Syst. Geohazards*. **9** (3), 128–147 (2015).
59. Yang, Q., Zhu, B. & Hiraishi, T. Probabilistic evaluation of the seismic stability of infinite submarine slopes integrating the enhanced newmark method and random field. *Bull. Eng. Geol. Environ.* **80**, 2025–2043 (2021).
60. Yang, S., Nadim, F. & Forsberg, C. F. Probability study on submarine slope stability. In: (eds Lykousis, V., Sakellariou, D. & Locat, J.) (Advances in Natural and Technological Hazards Research, Springer, 2007). 161–170.
61. Zhang, L. L. et al. Wave-induced oscillatory response in a randomly heterogeneous porous seabed. *Ocean Eng.* **111**, 116–127 (2016).
62. Zhu, B., Pei, H. & Yang, Q. Probability analysis of submarine landslides based on the response surface method: a case study from the South China sea. *Appl. Ocean Res.* **78**, 167–179 (2018).
63. Zhu, B., Pei, H. & Yang, Q. Reliability analysis of submarine slope considering the Spatial variability of the sediment strength using random fields. *Appl. Ocean Res.* **86**, 340–350 (2019).
64. Wang, Y., Wang, R. & Zhang, J. M. Large-scale seismic seafloor stability analysis in the South China sea. *Ocean Eng.* **235**, 109334 (2021).
65. Sultan, N. & Garziglia, S. 3D stability analysis of submarine slopes: a probabilistic approach incorporating strain-softening behaviour. *Landslides* **21**, 2695–2709 (2024).
66. Ceron, M. V., Cecilio, D. L., Linn, R. & Maghous, S. Face stability of shallow circular tunnels driven under the water table: A numerical analysis. *Int. J. Numer. Anal. Meth. Geomech.* **49**, 2459–2491 (2025).

## Acknowledgements

The authors gratefully appreciate the support provided by the Brazilian Research Council (CNPq) and the Brazilian Federal Agency for Support and Evaluation of Graduate Education (CAPES).

## Author contributions

JPCQ: Writing – original draft, Methodology, Formal analysis, Conceptualization, Investigation. SM: Supervision, Writing – review and editing, Methodology, Investigation, Conceptualization.

## Declarations

## Competing interests

The authors declare no competing interests.

## Reprints and permissions information

is available at [www.nature.com/reprints](http://www.nature.com/reprints).

## Publisher's note

Springer Nature remains neutral with regard to jurisdictional claims in published maps and institutional affiliations.

## Open Access.

## Additional information

**Supplementary Information** The online version contains supplementary material available at <https://doi.org/10.1038/s41598-025-31593-y>.

**Correspondence** and requests for materials should be addressed to S.M.

**Reprints and permissions information** is available at [www.nature.com/reprints](http://www.nature.com/reprints).

**Publisher's note** Springer Nature remains neutral with regard to jurisdictional claims in published maps and institutional affiliations.

**Open Access** This article is licensed under a Creative Commons Attribution-NonCommercial-NoDerivatives 4.0 International License, which permits any non-commercial use, sharing, distribution and reproduction in any medium or format, as long as you give appropriate credit to the original author(s) and the source, provide a link to the Creative Commons licence, and indicate if you modified the licensed material. You do not have permission under this licence to share adapted material derived from this article or parts of it. The images or other third party material in this article are included in the article's Creative Commons licence, unless indicated otherwise in a credit line to the material. If material is not included in the article's Creative Commons licence and your intended use is not permitted by statutory regulation or exceeds the permitted use, you will need to obtain permission directly from the copyright holder. To view a copy of this licence, visit <http://creativecommons.org/licenses/by-nc-nd/4.0/>.

© The Author(s) 2025